University
of Stuttgart

Institute for Materials Science

Chair of Materials Physics

High Resolution and Analytical Materials Microscopy

Seminar 2019

23th of September to 11th of October

Laboratory Instructions

Contents:

General remarks

- The presence in all of the lectures and laboratories is mandatory.
- This block course is a labor-intensive course which includes many important experimental techniques for materials scientists within a short period of time.
- Literature and a computer for open access during this block course can be found in the seminar room 2R10.
- Meeting point for the laboratories is at the offices of the experiment tutor (see next page).
- In the beginning of each laboratory session there will be a short colloquium. In case someone is not well prepared for the lab he/she will be excluded.
- Times for laboratory experiments:
  - Morning session: 9:00 am to 13:00 pm
  - Afternoon session: 14:00 pm to 18:00 pm
- **Regarding the experimental reports:**
  Purpose of the report is to document what was done during the class, to evaluate the results obtained and to answer the questions. The reports must be:
  - **Hand written**: (any images needed, you may print & glue them).
  - Each group has to hand in at least one handwritten report where all questions are answered (we expect all students to participate in the work on the report). Of course you are also allowed to hand in an individual report.
  - All members of the group have to sign the first page, approving the report.
  - Deadline is one week after the end of the seminar (18th of October).
- **Grading:**
  - 1/4 of the preparation
  - 1/4 lab day performance
  - 2/4 handwritten report

Experiment tutors

SUPERVISORS				
	LAB	**Tutors**	**Office**	**E-Mail**
Preparation				
1	Sputter/ WLI	Sebastian Eich / Ke Wang	2Q15 / 2Q14	sebastian.eich@imw.uni-stuttgart.de Ke.Wang@mp.imw.uni-stuttgart.de
2	EBSD Prep	Yoonhee Lee	2Q15	Yoonhee.Lee@mp.imw.uni-stuttgart.de
3	FIB liftout	Yug Joshi	2Q11	yug.joshi@mp.ime.uni-stuttgart.de
Characterization				
4	SEM / EDX	Sam Griffiths	2Q11	Samuel.Griffiths@mp.imw.uni-stuttgart.de
5	TEM	Robert Lawitzki	2Q11	Robert.Lawitzki@mp.imw.uni-stuttgart.de
6	TEM simulations	Franziska Maier	2Q11	Franziska.Maier@mp.imw.uni-stuttgart.de
7	EBSD	Dr. Gabor Csiszar	2Q17	Gabor.Csiszar@mp.imw.uni-stuttgart.de
8	APT-measur.	Ahmed Mohamed / Jianshu Zheng	2Q11	Zheng.Jianshu@mp.imw.uni-stuttgart.de Ahmed.Mohamed@mp.imw.uni-stuttgart.de
9	APT-reconstr.	Ruya Duran / Helena Solodenko	2Q11 / 2Q15	Rueya.Duran@mp.imw.uni-stuttgart.de Helena.Solodenko@mp.imw.uni-stuttgart.de

Time schedule

	Monday		Tuesday		Wendsday		Thursday		Friday	
Group	**23.09. morning**	**23.09. afternoon**	**24.09. morning**	**24.09. afternoon**	**25.09. morning**	**25.09. afternoon**	**26.09. morning**	**26.09. afternoon**	**27.09. morning**	**27.09. afternoon**
1				EBSD Prep	EBSD			TEM simulations		
2					TEM	TEM simulations		EBSD Prep		
3					Sputter/WLI			SEM / EDX		
4					SEM / EDX			Sputter/WLI		

	Monday		Tuesday		Wendsday		Thursday		Friday	
Group	**30.09. morning**	**30.09. afternoon**	**01.10. morning**	**01.10. afternoon**	**02.10. morning**	**02.10. afternoon**	**03.10. morning**	**03.10. afternoon**	**04.10. morning**	**04.10. afternoon**
1		Sputter/WLI		TEM			Official holiday			
2		EBSD				Sputter/WLI				
3		EBSD Prep		EBSD		FIB liftout				
4				APT-measurement		APT-reconstruction				

	Monday		Tuesday		Wendsday		Thursday		Friday	
Group	**07.10. morning**	**07.10. afternoon**	**08.10. morning**	**08.10. afternoon**	**09.10. morning**	**09.10. afternoon**	**10.10. morning**	**10.10. afternoon**	**11.10. morning**	**11.10. afternoon**
1		APT-measurement		FIB liftout	APT-reconstruction		SEM / EDX			
2		FIB liftout				APT-measurement	APT-reconstruction		SEM / EDX	
3				TEM	TEM simulations			APT-measurement	APT-reconstruction	
4		EBSD Prep			FIB liftout	EBSD	TEM		TEM simulations	

lectures

Ion Beam Sputtering

A working gas, in our case Argon, is inserted into a hollow volume inside the ion source. To be able to ionize this working gas the ionization energy has to be paid. Therefore, a helical 16 turn filament (Tungsten-Thoriumoxid), supported by two posts, is also mounted inside this volume. Applying a high DC current (2-3 A) heats the filament and starts the electron emission. Between filament (cathode) and cylinder wall the discharge voltage is applied, which accelerates the electrons to the outer wall (anode). On their way to the anode the electrons ionize the neutral working gas atoms by impact ionization. The positive ions are then accelerated to the cathode. Conductive plasma of nearly equal numbers of electrons and ions, in a background of neutral atoms is formed.

One of the cross sectional area contains the accelerator system, which is isolated from the rest of the cylinder. The accelerator system itself is made up of two isolated grids. The inner grid, called the screen grid, is on cathode potential and is used to focus the ion beam. Ions passing the screen grid are then accelerated by the accelerator voltage applied to the accelerator grid, the outer grid, and leaving the ion beam source. Outside the gun a neutralizer, another helical filament (45 turns), is mounted. The produced electrons provide space charge neutralization of the ion beam and prevent the build-up of damaging surface potentials on targets and substrates.

The ion beam hits the target and due to the collision atoms of the target material are evaporated. These atoms are deposited to some extent on the substrate which is oriented with the same angle towards the target as the incident beam is oriented to it. The deposition process is controlled in situ by a quartz crystal thickness monitor, which is mounted parallel to the substrate. The crystal is oscillating at given frequency. This frequency is changed when the mass of the crystal is changed. As one evaporates material onto the quartz crystal, its mass goes up and the frequency of oscillation goes down. This change is more or less linear and it can be calibrated in terms of frequency vs. deposition thickness.

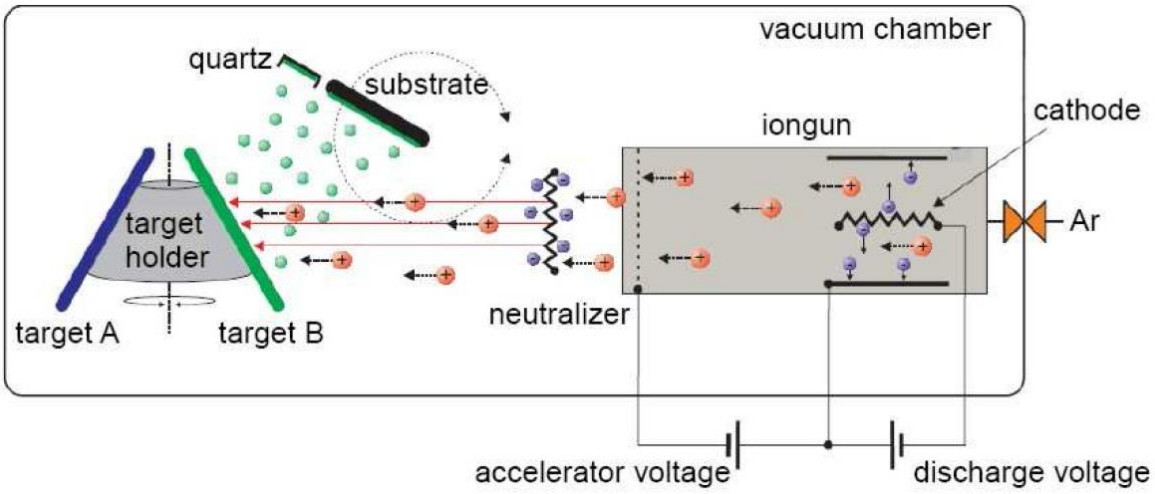

Figure 1: Schematical illustration of an ion beam sputtering chamber.

Sputter chamber 2 (step-by-step instructions)

1. Make sure everything is OFF on the electronic display (initially controls should be set to 0V/A).
2. Restart computer before using – DA convertor that gives signal to the gun gets confused if not
3. Put samples in the chamber!!! – **Without the argon flow on!!!!**
    a. When you put the samples in the airlock: Never open 1st and 2nd valves simultaneously.
    b. Sample into sample lock while valves ON OFF OFF). Close sample lock.
    c. Change valves to OFF OFF OFF, then OFF ON OFF!
    d. Then OFF ON ON when no noise is coming from the venting of the airlock.
    e. Then open black valve and put samples in, then close black valve.
    f. When done – close vacuum of the airlock! (OFF OFF ON)

-Sample holder: 360° for inserting / 45° for sputtering/180° substrates cleaning

4. SLOWLY, Open Ar valves for Neutralizer and Cathode (watch that pressure doesn't go too high)

-Pressure should go at about 10-5

5. Set Cathode and Neutralizer controller flow to approx. 2.5 sccm. Higher gas flow will help to ignite plasma, so 2.5 sccm is just a guide.

-Pressure now should be around 10-3.

6. Switch on DC GUN
7. Switch ON all switches **except** the neutralizer (controlled locally)

-Now discharge electrons from the cathode filament by heating it, and ignite the plasma by applying a positive potential to the discharge anode. If the cathode is broken, no current will flow through it.

-Create $V_{Discharge}$ --> Heat Cathode with I_{Cath} --> Attraction of thermally emitted electrons from Cathode Filament to Discharge Anode until $I_{Discharge} = 0.5$ A –> start filament: ignite at about $I_{Cath} = 9\text{-}13$ A depending on the form of the cathode and its age.

8. Discharge: -- ON (on the PC), Set to 70V and press SET
9. Cathode 'Heating Current' (on the PC), Set to 8A and press SET
   a. Set Discharge I to 0.5A and press SET

-WAIT until voltage and currents are stable. If $I_{Heating}$ goes above 13A without $I_{Discharge}$ increasing, press EMERGENCY STOP

-Beam --- acceleration between filament and accelerator.

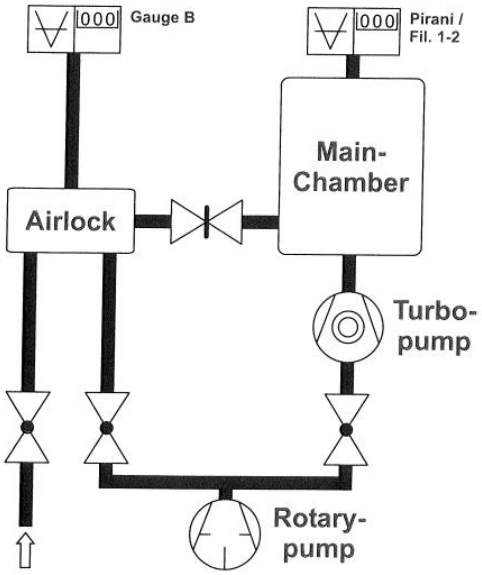

Figure 2: Vacuum circuit of sputter chamber 2.

10. Beam ON → *1000 V for cleaning Targets*
11. Accelerator ON → 100 V for all purposes → *make sure I_{Acc} as low as possible (0.1mA or less is good) → longer grid life!*
12. SET on PC Beam I=20mA .
13. On the electronics display: SWITCH ON neutralizer
   a. Increase the upper button until beam Current is about 1.5 x the beam current.
   b. The upper value should be larger than the lower value. If $I_{Heating}$ gets below 5mA, time to change the neutralizer filament.

-Keep an eye on discharge current to be at 0.5A

- IF I_{Acc} TOO HIGH: *can lower I_{Acc} by: Best option, lowering both Ar gas (not below 1.0 sccm and as long as beam and neutralizer are stable). If either beam becomes unstable, increase Ar flow again. Also lower I_{Beam} (but slower sputter rate). Or change V_{Acc} to 90V (not so helpful). If I_{Acc} is too high, maybe time to clean gun!!*

-We use a water cooling system – keeps the target at about 70C

OPERATIONAL PARAMETERS:

Target cleaning / Sputtering: **Beam voltage 1000V and 21mA**

If I_{acc} is too high: **Beam voltage 800V and 15mA**

Sample cleaning: **Beam voltage 600V and 10mA**

REMEMBER: Neutraliser current should be 1.5 x Beam current

-Increase the cathode current if plasma is not ignited!!! Discharge current will decrease below 0.5A CRITICAL!!!! Change the Ar flow in that case!!!!

After sputtering – Switch OFF

1. Put neutralizer to 0
2. Switch OFF neutralizer switch
3. On the computer screen:
   a) Select $I_{Heating}$ radio button. Press “fix” to fix actual current value.
   b) Switch OFF Accelerator

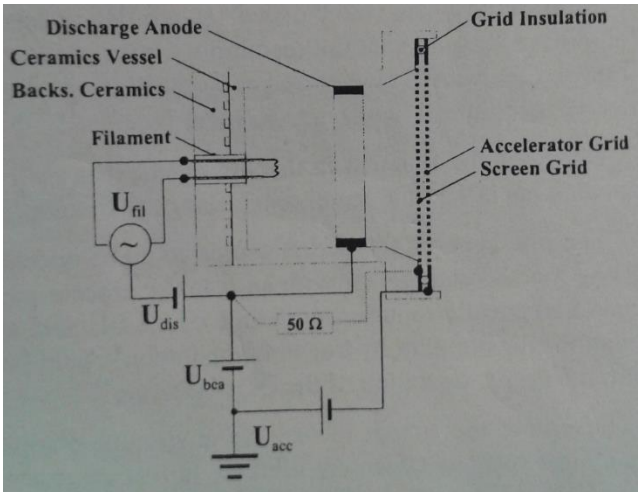

Figure 3: Wiring of the ion source and power.

   c) Switch OFF beam
   d) Set $I_{Heating}$ to 0.

e) OFF discharge current

4. OFF switches of the black controllers (MFC)
5. Switch OFF DC Gun
6. Decrease Ar neutralizer and cathode to 0 (unless cooling gun quickly)
7. Close argon valves on control panels
8. Close neutralizer to ZU
9. Close cathode to ZU

White-light Interferometer

The NewView is a scanning white-light interferometer. The instrument includes optics for imaging an object surface and a reference surface together onto a solid-state imaging array, resulting in an interference intensity pattern that is read electronically into a digital computer. A series of interferograms are generated as the objective is scanned perpendicular to the illuminated surface, while recording detector data in digital memory.

The data acquired in this way consists of an array of Optical System interferograms, representing the variation in intensity as a function of scan position. The interferograms stored in the computer are individually processed by FDA, and the final step is the creation of a complete three-dimensional image constructed from the height data and corresponding image plane coordinates.

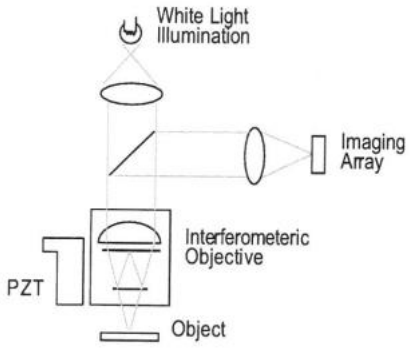

Figure 4: Optical system of the white-light interferometer.

Tutors:

Sebastian Eich und Ke Wang
Office: 2Q15/2Q14
sebastian.eich@mp.imw.uni-stuttgart.de +49 711-685-61981
ke.wang@mp.imw.uni-stuttgart.de +49 711-685-61983

Scanning Electron Microscopy (SEM)

Introduction

The basic principle of an SEM is depicted in Figure 5. The electrons are emitted from the filament/tip and a suppressor and an extractor electrode collect and funnel the electrons out of the source, through the first aperture and into the condenser where they are accelerated by a voltage of 1-50kV between the cathode and anode. The electron beam is demagnified by a two or three- stage condenser (magnetic lens) system, such that an electron beam of diameter 0.4-5 nm carrying a current of pA to µA is formed at the surface of the specimen [1].

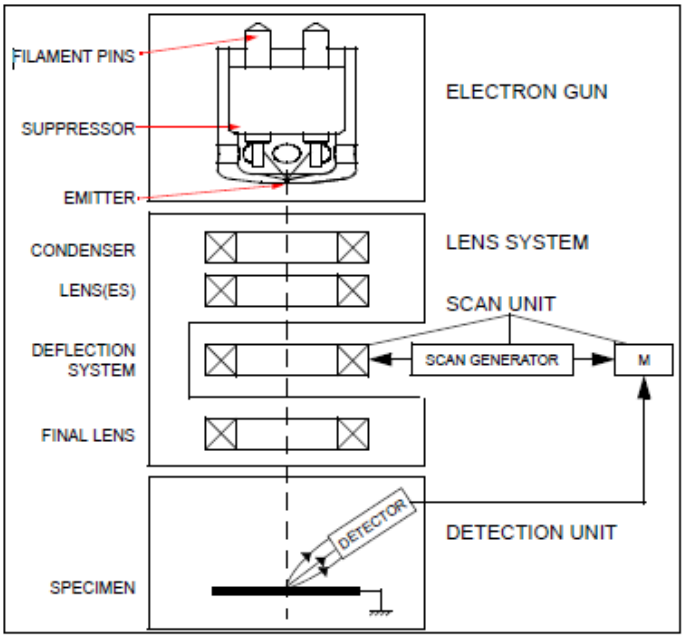

Figure 5: Schematics of an SEM.

A dual deflection coil system before the final lens scans the electron probe in a raster across the specimen which allows for the magnification of images by simple reduction of the deflection coil current. All scanned points on the x-y plane are displayed as a grey-scale pixels, where the detected intensities of scattered electrons leaving the specimen define the contrast.

Electron Emitters

Thermionic Emitters

Electrons in a cathode filament are thermally excited to overcome the work function of the material. The operating temperatures are between 2500-3000K for tungsten

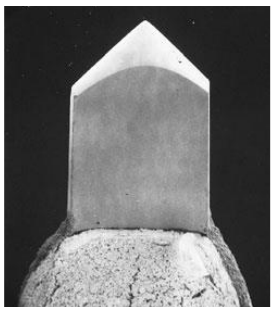

Figure 6: LaB_6 filament [2].

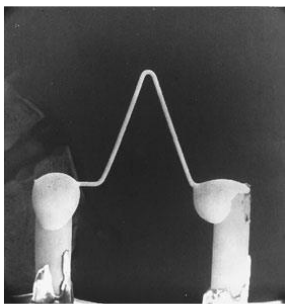

Figure 7: Tungsten filament [2].

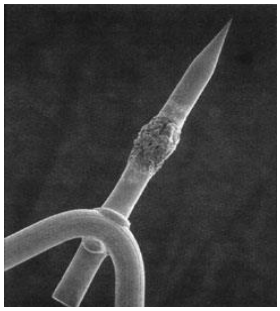

Figure 8: Field emission tip [2].

Figure 7 (and 1400-2000 K for LaB_6 Figure 6) due to a lower work function. These emitter are the cheapest, least bright and must be replaced regularly.

Cold field Emitters

Typically single crystal nanoscopically sharp tungsten tips (Figure 8). By applying a field of the order of 10^7V/cm between the tip and the anode, electrons are able to wave-mechanically tunnel from the filament into the vacuum. They produce the brightest beams and lowest chromatic aberration, but very high vacuum is required to avoid tip damage or contamination (e.g. by oxidation).

They can operate at room temperature but to avoid gas adsorption and to lower the at the tip the usual operating temperature is 1000K (Schottky type). The main advantage of these guns are much higher gun brightness.

Schottky Emitters

A compromise of the previous methods. A tungsten tip is coated with ZrO to lower its work function so that the operating emission temperature is much lower. This method has better emission brightness and chromatic spread than pure thermionic emission and while retaining long filament lifetimes.

Electron Optics

Electron Lenses

Electron lenses consist of an axial magnetic field with rotational symmetry. The electrons propagating through these lens systems are deflected in a screw trajectory due to the Lorentz force [1].

Lens Aberration

Spherical Aberration: If a parallel ray of electrons are incident on an electron lens, the electrons furthest away from the optical axis are focused closer to the lens. This is because the radial component of the magnetic field depends on the distance from the optical axis (OA), hence an electron traversing near the edges of the lens experiences a higher magnetic field, thereby getting focused to a higher point on the OA than the electrons traversing near the optical axis.

Axial Astigmatism: Magnetic inhomogeneity of the pole pieces, elliptical pole-piece bores and charging effects in the bore or at the aperture diaphragm cause asymmetry in the focusing field [2]. This asymmetry causes a different focusing field in two perpendicular planes, hence the electrons moving in these planes are focused at

different distances from the lens. A pair of quadrupole lenses can compensate this aberration.

Chromatic Aberration: The focal length of the lens depends on the energy of the incident electron and hence electrons with different energies are focused at different distances from the lens.

Focusing

The image can be focused by varying the current in the last pole-piece lens. It is advised to focus on specimen details at higher magnification to have good quality images at some lower magnification. If the image appears to be distorted in a particular direction, then the stigmator must be adjusted.

Detectors

The most effective detection system for secondary electrons (SE) is the Everhart-Thornley (E-T) detector. These consists of a positively biased grid placed in front a scintillator (converts electrons to photons by cathodoluminescence [2]) which is additionally biased at +10kV. E-T detectors can also be used to solely detect backscattered electrons (BSE) by applying a small negative bias to the screen grid to repel SEs. But such detectors have low efficiency due to a lack of geometrical optimization. Other alternatives for BSE are semiconductor detectors or BSE to SE conversion detectors. Passive Scintillator Backscattered Electron Detectors work without a scintillator bias. This is advantageous as only BSEs will have sufficient kinetic energy to be converted at the scintillator. Additionally the lack of an applied bias allows the detector to be positioned close to the sample without disturbing the primary beam, thus vastly improving detector efficiency.

Beam-Specimen Interactions

As the SEM primary beam is scanned across a specimen surface, it penetrates the surface and scatters randomly, losing its energy due to gradual dampening within a volume known as the *interaction volume*.

Interaction Volume

Once the electrons of the primary beam penetrate a specimen, a cascade of elastic and inelastic electron-specimen interactions are initiated. Elastic scattering of electrons occurs at atomic nuclei and causes the divergence of the primary beam within the specimen. Inelastic interactions (electron-electron scattering, photoelectric effect), which also contribute to beam divergence, more strongly contribute to dampening of

the primary beam energy and hence primary beam penetration depth, where the dampening rate is strongly dependent on the material density and permits typical interaction distances between 10 nm – 10 µm. While traversing through the specimen, electrons of the primary beam scatter repeatedly until they either exit the specimen as transmitted or 'back-scattered' electrons, or flow as current to ground (conducting specimens) or are accumulated as charge on the specimen surface (insulating specimens). Specimen 'charging' causes deflection of the incident primary beam which results in reduced imaging quality. Often, insulating samples are sputter-coating with an ultrathin layer of a dense metal (e.g. Pt, Au) [1] to facilitate charge flow. Some SEMs offer the function to introduce low pressure gas into the specimen chamber can also reduce charging, but reduces the beam resolution.

Electron-electron Interactions

The elastic electron-electron scattering events which occur under the surface of an SEM sample are critical for the imaging of the specimen surface. Primary electrons (PE) entering the specimen are scattered by shell electrons of the specimen material, transfering kinetic energy [2].

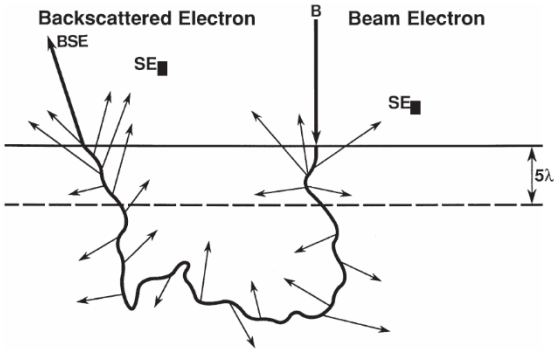

Figure 9: Formation of backscattered (BSE) and secondary (SE) electrons. λ is the SE mean free path [2].

Atomic electrons which ionise from the outer shell during this process are called **secondary electrons**. SE are the primary source of topological information for SEM imaging since they represent the larger portion of measurable electrons and due to their low kinetic energy (≤50 eV) can be easily collected at the SE detector using a positive bias collector grid. The SE detector is positioned above and to the side of the specimen to improve contrast, where the increased electron collection on the specimen detector side appears as illumination. Due to their low energy, SEs only exit from the top few nanometers of material.

BSE which originate from the primary beam, in contrast to SE, exit the specimen with much higher kinetic energies (keVs). Thus, BSE are detected leaving a larger exit volume. High energy BSE cannot easily be collected using a positive bias, so BSE detectors are typically positioned directly above the specimen around the beam column where maximum BSE are collected. Negatively, due to the larger exit depth, BSE exibit worse resolution at higher magnifications. Although because higher $\bar{Z}$ number regions scatter more strongly, better contrast than for SE are achieved over regions with a $\bar{Z}$ gradient [1].

X-ray Emission (most relevant for EDX):

When inelastic electron-electron interactions occur, often electromagnetic radiation is emitted, where conservation of energy must be satisfied [3]. This can occur in one of two ways:

Bremsstrahlung – A PE can be deflected and decelerated by a shell electron causing the PE to emit an x-ray with energy dependent on the loss of kinetic energy. An entire spectrum of Bremsstrahlung is characteristic and indicative of the statistical nature of electron deflections (i.e. kinetic energy loss).

Characteristic x-rays – When a shell electron is ionized by a PE, the atom is left unstable and soon after the empty energy level is filled by an electron from a higher level. The shift of the electron to a lower energy level results in the emission of an x-ray of energy characteristic both of the element and the electron shell transition. Hence, characteristic x-rays are used in EDX to determine the composition of a specimen and are annotated with Siegbahn notation. E.g. Cu Kα = 8.040 represents an electron transition in a Copper atom from the L shell to the K shell.

Using an SEM

Key Words

Working Distance: It is the distance between the specimen and lower pole-piece. ***Eucentric Point:*** Where the focal point lies on the tilt axis. ***Beam Shift:*** Adjusting the electron beam scan area without moving the sample stage (i.e. with lenses).

Procedure

1. Sample preparation: Be sure that your samples are conductive. The samples should be mounted on aluminum pin stubs using either a conductive glue (silver glue) or carbon tape. If the samples are insulating a conductive contact needs to be established with the stub.
2. In standby condition, the microscope column is kept in vacuum (to avoid contamination). Once the samples are prepared, the sample lock can be vented and the sample/s placed in the stub holder.
3. An image of the sample stage is taken for navigation and the chamber is closed and pumped.
4. Wait for the vacuum to reach the operating pressure.

5. Start the electron gun. Find and focus the e-beam on the highest point of your sample then link the relative z-height of the column to this point (IMPORTANT SAFETY PRECAUTION).
6. Bring the sample to the working distance (10mm for FEI Quanta) and focus, link, and adjust the height again.
7. Now the SEM is in working condition and could be used for various applications.

NOTE: certain detectors are optimized for a particular working distance (e.g. X-ray detector). Read the manual for specific type of detector.

To take the samples out, first switch the beam OFF, lower the stage and vent the chamber.

Experimental

1. A sputter-coated biological sample will be investigated while learning to operate the SEM (sample prep/loading, WD, focusing, astigmatism, beam shift, tilting).
2. Topographical analysis of a high entropy/super alloy comparing SE and BSE imaging modes. Chemical Analysis using EDX.
3. A sample cross-section will be analyzed with EDX to determine the cross-sectional composition gradient. Preparation of the sample to limit sample charging.
4. Sputtered alloy layers of differing thickness will be analyzed with EDX to determine the composition of the alloy, as well as a correction factor for the absorption error.

Tasks for the report:

1. Report on the experimental procedure: include what have you done and why, using practical and theoretical reasoning. (1-2 pages).
2. Conduct size and/or distribution analysis of particles/precipitates of an SEM images using ImageJ (FIJI) freeware (or similar software). Image taken by students during the course.
3. Index 1-2 EDX spectra using Siegbahn notation. Additionally define the meaning of Siegbahn notation based on quantum numbers and electron energy levels.
4. Using a sample with known constituents, evaluate an EDX line scan to determine which phases are present. Indicate which phases are present at all

positions on the line scan. If the compositions do not match any phase precisely explain why.

5. Considering that EDX spectra corrections can be split into signal corrections and matrix (material) corrections:
    a. Define the most important signal corrections required for EDX analysis including detector corrections.
    The following equation is used to calculate the concentration of an element from the intensity of an EDX spectra:
    $C_i^{samp}/C_i^{std} = [ZAF]_i \cdot I_i^{samp}/I_i^{std} = [ZAF]_i \cdot k_i$
    b. Explain the utility of the *k*-factor. Explain the individual components of the ZAF matrix correction. Give examples of samples which would require a large correction in each case, justifying why. What are the advantages and disadvantages of standard vs. standard-less EDX analysis and which type of analysis was used during the lab course?
6. Using Fe-Al sputtered samples of the same composition but differing layer thickness, compare the at. % value as determined by the EDX software and explain why there is a deviation based on the ZAF factor (1/2 - 1 page). Approximately how deep is the interaction volume in this alloy?
7. How does the heterogeneity of a sample effect the accuracy of its EDX analysis?

References

[1] L. Reimer, Scanning Electron Microscopy: Physics of Image Formation and Microanalysis - Second Edition, Berlin: Springer-Verlag, 1998.

[2] J. Goldstein, D. Newbury, D. Joy and C. Lyman, Scanning Electron Microscopy and X-Ray Micro analysis, New York: Springer, 2003.

[3] J. Thomas and T. Gemming, Analytische Transmissionselektronenmikroskopie, Wien: Springer-Verlag, 2013.

Tutor:

Samuel Griffiths
Office: 2Q11
Samuel.Griffiths@mp.imw.uni-stuttgart.de +49 711-685-61905

Transmission Electron Microscopy 1 (TEM): Basics

Pre Information

During this seminar, a Transmission Electron Microscope (TEM), more precisely a Philips FEG CM200 will be used. You will be asked to operate the tool, and by this, learn how a TEM is functioning and how it is used in many materials science laboratories. In part 1 (not experimental), a quick review will be given on the basic principles on which electron microscopy relies. Then a more detailed description on high resolution transmission electron microscopy (HRTEM) and its limitations will be given. In part 3, you will learn more about the analysis and ex-situ simulations in order to be able to correctly interpret your TEM data. If you are not familiar to the basics and the operation of a TEM, you should study this chapter thoroughly, otherwise you can directly jump to part 2 HRTEM.

Quick Introduction

The wave-particle duality has been enunciated by Louis De Broglie in 1924. He predicted that every particle should also behave like a wave. Three years later, two different labs proved him right by passing an electron beam through a metallic thin film and observing a diffraction pattern. This discovery, in conjunction with the invention of electromagnetic lenses by Hans Busch in 1926, permitted the creation of a brand new kind of microscopes, using electrons instead of light. The first TEM was built by Ernst Ruska in 1937 (he was awarded half a Nobel Prize for this invention in 1986).

But why building such a tool in the first place? What is the advantage of using electrons with respect to light? The answer is given by the Rayleigh Criterion, which shows that the resolution of a microscope is mainly determined by the wavelength of the radiation it uses (as approximation the resolution is equivalent to this wavelength). In a visible light microscope, the wavelength of the radiation is between 400 nm and 700 nm. The goal of a TEM is to produce an electron beam with much smaller wavelength, in order to see much smaller features.

What is the typical wavelength of an electron in a TEM?

De Broglie, in his PhD thesis, originally stated that the wavelength of a particle is given by

$$\lambda = h/p \quad , \tag{1}$$

where h is the Planck constant and p the momentum of the particle.

In the case of an accelerated electron, λ becomes

$$\lambda = \frac{h}{\sqrt{2m_0 Ue}} \quad , \tag{2}$$

where m_0 is the rest mass of an electron, U the acceleration voltage, and e the elementary charge of an electron.

A typical acceleration voltage in a TEM is 200 kV. This leads to a theoretical value of λ = 2.73 pm. (Already 100 000 times less than visible light). Since electrons are moving quite fast under this acceleration voltage (the velocity of an electron accelerated by 200 kV is around 2.086×10^8 m/s), it is more accurate to take into account relativistic effects and to change equation (2) into

$$\lambda = \frac{h}{\sqrt{2m_0 Ue\left(1+\frac{Ue}{2m_0 c^2}\right)}} \quad . \tag{3}$$

The corrected wavelength of an electron is then λ = 2.51 pm. This means that the features possible to see in a TEM should be much smaller than in a visible light microscope. Actually this means subatomic features can be observed (typical size of an atom is 1 Å ≡ 100 pm). Obviously this performance cannot be achieved, but this statement itself is sufficient to explain why Ernst Ruska tried hard to build the first electron microscope.

Structure, Operation and Alignment of a TEM

With the arrival of full computer control, the operation of the microscope has become much easier, especially in those modes where before, considerable operational experience was required to get results. A logical consequence has been the increase of the operators of a TEM. In our days, not only experience and dedicated microscopists use a TEM, but also life scientists, who do not have a deep-rooted knowledge of electron microscopy, but simply use the instrument as a tool for their studies. For high performance use of the microscope a number of alignments are required. Additionally, some of the alignments are actually only important for the ease of use and have no effect on the microscope performance. The “DIF ALIGNM” in our TEM for instants aligns the diffraction patterns at all camera lengths, so that it is not necessary to decenter the diffraction pattern each time the camera length is changed, which is convenient but has no effect on the quality of the diffraction patterns. Modern technology guarantees high stability of the alignment. Instead of using potentiometers that are prone to drift with time the TEM is digitally controlled, ensuring this way a higher degree of stability. Furthermore, the alignments can be stored and recalled into

the microscope when needed. Once fully aligned, the microscope requires only a minimum of adjustment before use, mostly for high resolution imaging.

The alignment is not particularly difficult to do, but understanding what happens in each step is the challenge. This and the function of the most important parts of a TEM will be explained in the following.

Electron gun: the electron beam is produced in the electron gun (also called cathode). Two basic types of guns can be distinguished. A) the thermionic gun, based on 3 types of filaments: W, LaB_6, or CeB_6, whose lifetime is pretty short, and b) the field emission gun (FEG) which employs either a thermally-assisted cold field emitter or a Schottky emitter (which is the case in our TEM). Table 1 gives an overview of the most important parameters of these different types of guns.

Table 1: Parameters of the different types of guns for an easy comparison. The difference in brightness, stability as well as working temperature is important.

	W	LaB_6	CeB_6	CFEG	TCFEG	Schottky
Temperature (K)	2700	2000	2000	300	1800	1800
Energy spread (eV)	3-4	1.5-3	1.5-3	0.4-0.8	0.8-1.5	0.6-1.2
Brightness (reduced)*	1	10-30	10-30	500-5000	500-5000	2500
Source size (nm)	$3 \cdot 10^4$	$5 \cdot 10^3$	$5 \cdot 10^3$	3	3	20
Maximum current (nA)	1000	500	500	30	30	300
Stability (%)	<0.1	<0.1	<0.1	2-10	1-5	0.1

* the reduced brightness (A cm^{-2} $srad^{-1}$), the real brightness divided by the accelerating voltage (in volts), makes it possible to compare directly between microscopes operating at different voltages.

FEG requires a different gun design than the thermionic gun, as well as a much better vacuum in the gun area (10^{-8} Pa instead of 10^{-5} Pa). It is therefore more expensive; however, it offers a much better quality of work. The FEG consists of a small single-crystal W needle that is put in a strong extraction voltage (in our case 3.95 kV). In the case of a cold FEG the needle is so sharp that electrons are extracted directly form the tip. For the Schottky FEG a broader tip is used which has a surface layer of zirconia (Figure 10) which mainly lowers the work function. A characteristic of a FEG is that the electron trajectories seemingly originate inside the tip itself, forming a virtual source of electrons for the microscope, and therefore a more coherent electron beam that will allow better resolution later on.

Once they are extracted from a material, electrons are accelerated towards the sample. Acceleration is achieved by applying a high voltage (typically 200 kV) between the cathode (the source) and an anode.

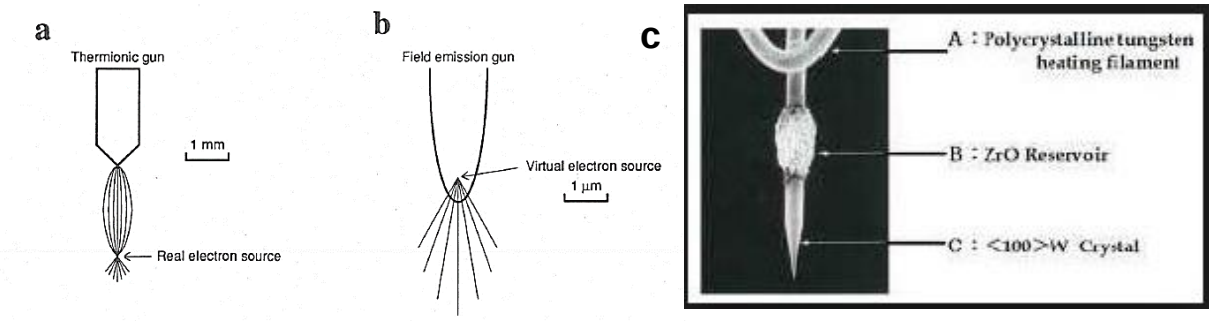

Figure 10: a) Schematic diagram of the real source of a thermionic gun and b) the FEG showing the virtual source of the electrons, c) the tip of a Schottky FEG, with a layer of zirconia around tungsten.

To sum up, the high main benefits of a FEG are: 1) the small size of the tip ensuring a large number of electrons to be emitted from a small area (high A/cm^2) with the same energy and 2) electrons come out of the W tip with a very restricted range of emission angles (high A/srad). FEGs therefore have a low energy spread.

Since now, a description about why it is interesting to use electrons, and how an electron beam is generated has been given. The importance of using a FEG and the different components of the gun. Now let us see how the beam is focused and handled.

Lens: The beam is focused on the sample using a set of lenses and apertures. The part of the TEM containing the lenses and the sample is called the column. The lenses in a TEM are electromagnetic lenses (with only exception the gun lens in the FEG which is an electrostatic lens). Those lenses have the same function as lenses in a visible light microscope; however, they are working slightly different. These lenses all consist of a coil, through which an electrical current flows, creating a magnetic field inside the microscope that affects the paths of the electrons. An electron going through such a magnetic field will be deviated (Lorentz force) according to the strength of the magnetic field. Changing the current through the lens coil changes the magnetic field and thus the strength of the lens. The TEM usually contains of two condenser lenses. First is the **C1**, determining the demagnification (size reduction) of the electron source onto the specimen and thus the spot size (you can control this when changing the spot size knob which has 11 steps). The second condenser lens, called **C2** determines how strongly the beam is focused onto the specimen. As a consequence, it varies the intensity of the beam on the viewing screen. (This is controlled through the INTENSITY knob on the left side of the tool). Inside the C2 there is an aperture, called the **condenser aperture**, which is used as a beam defining aperture. It limits the amount of the beam convergence for a fully focused beam.

The magnification system of the microscope consists of a set of 5 lenses: the objective, diffraction, intermediate, projector 1 and projector 2 lenses. Except in LM

(low magnification) mode, the ***objective lens*** is always ON, and is the strongest and most important lens in the microscope, magnifying between 20 and 50x. The individual lenses of the magnification system are not controlled directly by the operator, but instead the microscope contains a number of magnifications for image and diffraction mode, each with its own settings of the magnifying lenses. The only lenses that are controlled directly by the operator are the objective lens and the diffraction lens for focusing the image and the diffraction pattern, respectively. The magnification is eventually achieved by a complex interplay between all the lenses.

Deflection coil: Throughout the microscope, the path of the electrons is affected by a number of deflection coils, mounted in different locations. Gun tilt and gun shift, beam tilt and beam shift, image shift and diffraction pattern shift are all controlled by the deflection coils. In its simplest form, a deflection coil is a set of two wires running parallel to each other on either side of the electron beam. If one wire is given a positive charge the other one is negatively charged, so that electrons in the beam will be attracted by the wire with the positive charge, and repelled by the one with the negative charge, leading to a deflection towards the positively charged wire. The actual design is somewhat more complicated, using a magnetic field generated by coils that are extended over 120°.

Each microscope has three sets of double deflection coils: the gun coils just underneath the electron gun, the beam deflection coils above the objective lens, and the image deflection coils below the objective lens.

The deflection coils play an essential role in the alignment of the microscope and are used for aligning the gun, the beam, the objective lens, the magnification system (image to the screen center), and the detector alignments. Most of the alignment procedures either align the deflection coils themselves or use the deflection coils to align another electron-optical element.

Here are some fundamental explanations and information concerning the alignment of a TEM:

1. **Specimens for alignment:** In principle the microscope alignment can be performed on the basis of any specimen that is electron transparent (thin enough). But a few types of specimen are particular useful (e.g. containing amorphous regions).
2. **Eucentric height:** What defines the correct z-position of a specimen? Thinking about it, there is nothing that stops you running the microscope with the specimen placed higher or lower relative to the objective and condenser lenses. However, there is a perfect z-distance where the TEM manufacturer has set up the ideal focus if the lenses. You find this point by moving the sample in z direction while tilting the specimen until there is a minimal movement of the image. This is called the eucentric height, which

means 'the height of the specimen at which its image does not moved laterally as a function of specimen tilt'. It is common practice to adjust the z-shift so that the middle of the specimen lies on the rotation axis of the specimen loading arm. This has the convenience of meaning that when the specimen is tilted, the point you are observing remains stationary.

3. **Pivot Points:** Double deflection coils are capable of two completely independent actions, a tilt and a shift. Those two actions should be decoupled, meaning, when a shift is intended only a shift and no tilt should occur. A pivot point is simply a point around which the beam will pivot. The alignment of the pivot point determines the relation between the two coils used, like on a kids' seesaw. Setting the pivot points is done by deflecting the beam with a wobbler and minimizing any movement of the beam. **A wobbler** is a mechanism for rapidly switching a microscope element or function from a negative value to an identical but positive value. Pivot points should be aligned at the beginning and at the end of the alignment with a perfectly focused sample.
4. **Gun alignment**: **(Tilt)** The gun tilt makes sure that the electron beam coming from the gun is parallel and centered to the optical axis, so that no electrons from the beam are lost before they can be used for imaging. The gun tilt is set by simply maximizing the intensity of the beam.
5. **Gun alignment**: **(Shift)** The gun shift alignment involves centering the beam for spot 9 (with SHIFT) and switching to spot 3 (using MULTIFUNCTION knobs) and centering this spots. (these two spot sizes are chosen because this minimizes the overall spot shifts as a function of a spot size. When the C1 lens is weak (spots 1-3) the gun shift positioning and repositioning is not accurate due to hysteresis. When there is a beam shift, when the spot size is changed, this is an indication that the shift alignment is not good. This alignment is not needed when the spot size is not changed later.
   Because of the importance for objective-lens alignment it is essential that beam shift and tilt are pure, and that is why they are aligned at the beginning of every use.
6. **Rotation Center:** If the image moves during focusing, a ROTATION CENTRE ALIGNMENT is required. The objective lens field needs to be centered to the optical axis. It can be chosen between high tension modulation and objective lens current modulation. FOCUS STEP SIZE can change the strength of the modulation.
7. ***The higher the magnification where the alignment is performed, the better the image quality will be.***
8. **Condenser C2 aperture:** The C2 aperture is aligned without a specimen inserted. If the C2 is not aligned, then the illuminated area is changing when varying the intensity of the beam. To align the aperture just turn the INTENSITY knob during wobbling of the intensity until the center of the illumination is fixed.
9. **Astigmatism correction:** Even though considerable effort is spent in order to ensure high lens quality, none of the lenses in a microscope is 100% perfect. Small inhomogeneity remains or comes even by changing the specimen itself. These imperfections cause a loss of rotational symmetry of the lens. In one direction the lens will therefore focus more strongly than in the perpendicular direction, causing an asymmetry called astigmatism. This can be corrected by using the STIG knob.
   Most microscopes have three sets of stigmators: the condenser stigmator, placed below the C2 in order to correct its errors and make the focused beam circular (before the specimen), the objective stigmator placed under the objective lenses in order to correct astigmatism (after the specimen) in the HM image and the low angle diffraction

patterns. Lastly the diffraction stigmator to correct astigmatism in the diffraction pattern and the low magnification imaging.

If HRTEM is performed, the objective stigmatism has to be aligned as well. The most simple way to do so is using an amorphous sample align the objective STIG by using the FFT image.

Fast Fourier Transformation (FFT) is the representation of the crystal in the reciprocal space. Effectively, it is a representation of the distribution of image spacings. Any distance visible in the image, becomes a pixel in the FFT. When an amorphous specimen is used, with many different spacings in all directions we observe a representation of the contrast transfer function. When there is no astigmatism the FFT will show concentric circular rings, but with astigmatism present the rings become elliptical.

The main aim of using a TEM is to obtain micrographs of samples at high magnifications. As previously mentioned, the idea of using an electron source was coming from the fact that a better resolution than with visible light can be obtained. But as already explained, a major problem is always present: electromagnetic lenses are far from being perfect.

Mainly two phenomena will decrease the resolution in a TEM:

- **The Chromatic aberration:**
  This will appear if the beam is not perfectly monochromatic (energy spreading of the electrons). The beams will have different focus points, leading to a loss of resolution. Possible *to correct by using a more coherent electron source (a FEG for instance) and a very thin sample (after going through a thick sample, electrons suffer inelastic interactions, leading to an energy spreading).*
- **The Spherical aberration:**
  The more painful aberration of the two, which means that electrons passing through a lens not exactly in the center will be focused at a different points. *This aberration, which is really easy to correct in an optical microscope (just requires an extra lens), is extremely hard to correct in a TEM and requires a complex setup of additional lenses supported by a fast computer to perform the corrections*

Imaging Modes

What about the contrast in TEM imaging? Interpreting a TEM image can be tricky. Any TEM will be affected by mass-thickness contrast and diffraction contrast. Thickness contrast arises from incoherent elastic scattering of electrons that go off axis. As the thickness of the specimen increases the elastic scattering also increases since the mean-free path remains fixed. Similarly, the higher the Z number of an element, more electrons will be scattered. This will create a difference in the intensity in an image,

where thicker samples or heavier elements will create more scattering and therefore less electrons will be transmitted to the image, giving a weaker direct image. Diffracted electrons leaving the surface of a crystalline specimen are intercepted by the objective aperture and prevented from contributing to the image. Alternatively, only one diffracted beam forms the image, giving this way information about the structure of the specimen.

Bright Field - BF

If the objective aperture is placed in the column axis (Figure 11 A), only electrons which are not scattered make it to the phosphorous screens. The aperture only lets the primary beam through. In a polycrystalline sample, this means that only those electrons that transmit grains which are not oriented in Bragg's condition will reach the screen (bright area). However, the electrons which are going through well oriented grains will be diffracted and will not reach the screen (dark area). This is called bright field imaging.

Dark Field - DF: (centered DF and displacement aperture)

The other possibility is to place the aperture away from the column axis (Figure 11 B). Then the reverse situation takes place. Only electrons coming from a diffracted area will be allowed to reach the screen, producing a bright contrast. This is called dark field imaging. However this may give a poor quality image since additional spherical aberration and astigmatism are present when the electron path is not close to the optic axis. In order to keep the resolution as good as in the BF mode, the beam is tilted so that the diffracted electrons travel along the optic axis. (Figure 11 C). This tilt is caused by using electromagnetic beam tilt device. Both DF cases will be discussed during the lab.

Diffraction Mode

Operating a TEM in the diffraction modes allows us to get information about the crystal structure of a sample. In the same way X-Rays are diffracted by a crystal, an incident beam of electrons will interact with its lattice planes. When the lattices planes are well oriented with respect to the beam (in a TEM, the beam has a constant orientation, the sample is moving), constructive interactions will produce diffraction spots. By tuning the intermediate lens properly, a diffraction pattern is displayed on the phosphorous screen representing a samples crystal structure in reciprocal space. Details about Bragg's Law and the selection rules will not be given here, since this is done during the semester TEM lab-class. You are however required to be familiar with those.

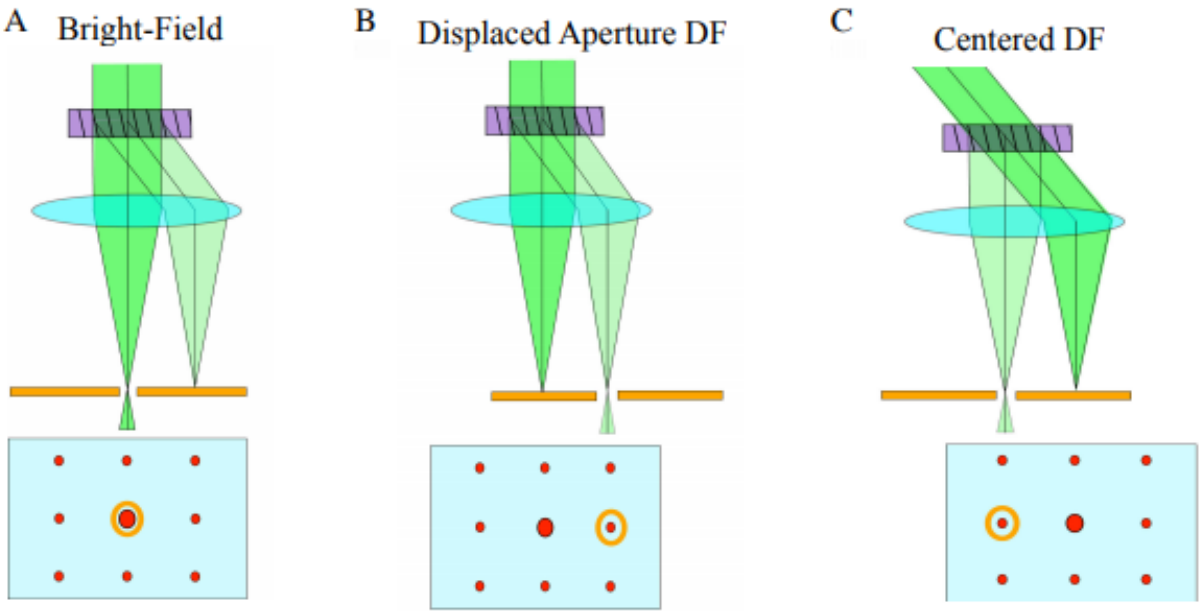

Figure 11: Diffraction contrast in TEM direct imaging.

Recommended literature to read

[1] D B. Williams and C. Barry Carter. Transmission electron microscopy: a textbook for materials science. New York, Spinger, 2009.

[2] L. Reimer, H. Kohl Transmission electron microscopy: physics of image formation New York, NY: Springer, 2008

[3] B. Fultz, J. Howe Transmission electron microscopy and diffractometry of materials. Berlin; New York: Springer, 2008

[4] J Bozzola; L D Russell. Electron microscopy: principles and techniques for biologists. Boston, Jones and Bartlett, 2006.

Transmission Electron Microscopy 2 (TEM): HRTEM

Introduction

In this part of the microscopy lab, we will focus on the information limits of a TEM, which can lead us to magnifications of up to 1 000 000 x enabling the ability to resolve atomic columns of a crystal (e.g. silicon). Here, we will use a combination of monocrystalline Si, amorphous Si and polycrystalline Al to study the most important topics of high resolution transmission electron microscopy (HRTEM).

In order to be capable of interpreting and understanding high resolution images, the following theoretical considerations have to be taken into account:

Phase contrast:

To create a reasonably good image, not only high resolution is necessary, but respective contrast mechanisms as well. Scattering absorption contrast, which is dependent on the mass thickness, as well as diffraction contrast, which is dependent on different crystallographic orientations, are mainly responsible for overall image contrast at lower magnifications. None of the two mentioned contrast mechanisms can be applied, if one considers to image a monocrystalline sample at high magnification. Thus, a 'further' contrast mechanism must be taken into account as soon as we work with high resolution images. Therefore, the wave-particle duality of an electron and the respective interaction mechanisms with a periodical crystal lattice have to be considered. In relation with the Schrödinger-equation, the wavelength of an electron λ_{Kr} within a potential Φ (e.g. the potential of an atom or a crystal lattice due to charges) can be calculated as:

$$\lambda_{Kr} = \frac{h}{\sqrt{p^2 + 2 \cdot m \cdot e \cdot \Phi}} \tag{4}$$

With *h*: Planck's constant, *p*: electron momentum, *m*: electron mass, *e*: elementary charge. In a non-relativistic approximation the electron momentum can also be written as:

$$p^2 = 2 \cdot m \cdot e \cdot U_B \tag{5}$$

Whereas U_B is the acceleration voltage. Summarizing both equations we end up with:

$$\lambda_{Kr} = \frac{h}{\sqrt{2 \cdot m \cdot e(U_B + \Phi(x,y,z))}} \tag{6}$$

The potential Φ becomes zero as soon as the electron does not pass through the crystal, which has a dramatic consequence: The wavelength of electrons is shortened as soon as a crystal lattice is being crossed, causing a phase shift $d\phi$ within a crystal thickness dz. In other words: the phase shift $d\phi$ represents the periodicity of the crystal lattice, as shown in Figure 12:

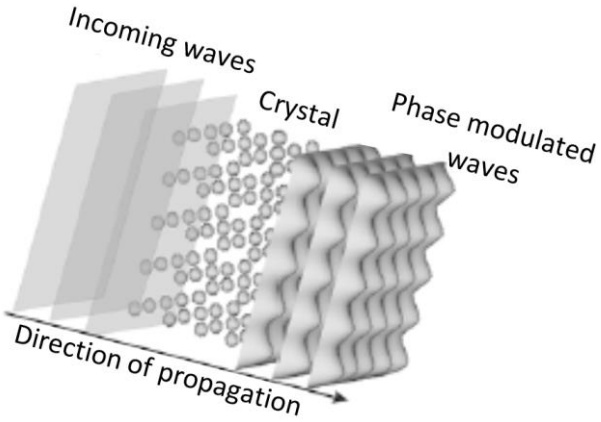

Figure 12: Phase modulation of electron waves through a crystal lattice.

In order to use the phase modulation of the electron waves through a crystal lattice, the phase shift of two incoming electron waves has to be chosen in a way that it causes amplification. Thus an amplitude modulation can be created out of a phase modulation, meaning that (for example) crystal positions with a higher potential Φ appear brighter than positions with a lower potential Φ: In the case of a very thin, defect free and well aligned sample (in beam direction) it is possible to resolve single atom columns.

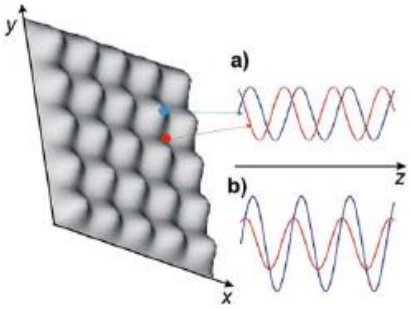

Figure 13: Conversion of a phase modulation into a amplitude modulation. The case b) shows amplification after interference with a wave with the same phase shift.

Low indexed lattice planes of a crystal are the best choice to see atom columns clearly, since the distances between the respective columns appear the largest. To obtain the correct zone axis of the monocrystal, you will make use of Kickuchi-lines in the

diffraction mode. If you do not know what Kickuchi lines are or forgot about their theoretical origin, we encourage you to study this topic in more detail using the books available in the seminar room.

Contrast transfer function and Scherzer focus

Since we now know that phase contrast plays an important role for the image interpretation in HRTEM, we would now like to know how this contrast is transferred through the objective lens. To get a further insight consider Figure 14:

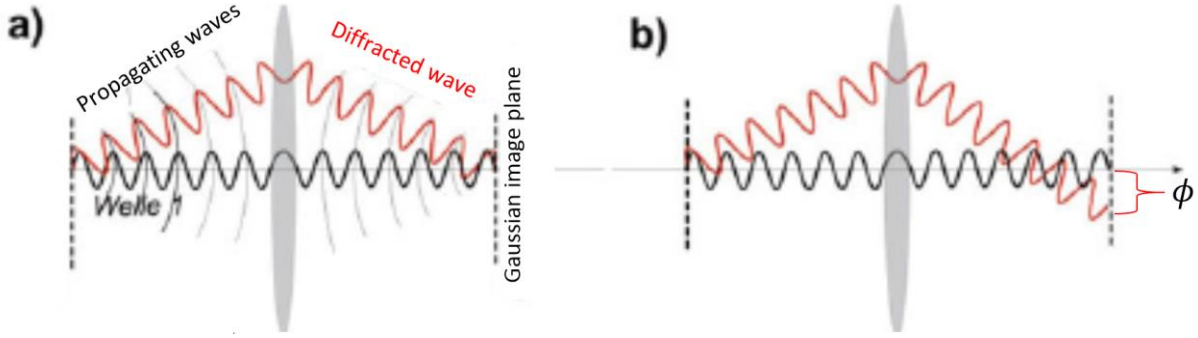

Figure 14: Wave-interference after interaction with the lens: (a) in the ideal case (b) with a phase-shift in the Gaussian image plane. (The diffracted wave is scattered by the specimen.)

The phase shift ϕ shown in Figure 14, can be either caused by spherical aberration or by defocussing. Since the strength of the focal length can be tuned, we can defocus on purpose in order to obtain a phase shift and thus an amplitude modulation: We need to defocus in order to be able to resolve atomic columns. The third important influence parameter on the phase shift ϕ is the diffraction angle θ. According to Bragg's law, the diffraction angle is related to the reciprocal length as:

$$\theta \sim \frac{1}{d} = q \tag{7}$$

With *d* as the lattice plane distance and *q* as the spatial frequency. Therefore the phase shift ϕ is depended on:

$$\phi = \phi(q, \Delta f, C_S) \tag{8}$$

Whereas Δf represents the defocus and C_S the spherical aberration constant. The dependency on the phase contrast, and thus on the image contrast, can be well approximated by the contrast transfer function CTF:

$$CTF(q) = \sin\left(\frac{\pi}{2}(C_S \cdot \lambda^3 \cdot q^4 - 2 \cdot \Delta f \cdot \lambda \cdot q^2)\right) \cdot e^{-\pi^2 C_C^2 \left(\frac{\Delta E}{E_0}\right)^2 \lambda^2 q^4} \tag{9}$$

In which C_C denotes the chromatic aberration constant. The exponential term represents a damping factor. We can easily see that the best 'contrast transfer' (e.g. the highest spatial frequency q, for which images are easy to interpret) is achieved with a slight defocus Δf, since the influence of the spherical aberration constant C_S on the CTF (in the sinoidal term) is reduced. Solving equation (9) for $|q_{max}|$ and certain approximations lead us to the so-called 'Scherzer focus' Δf_{Sch}

$$\Delta f_{Sch} = 1{,}2 \cdot \sqrt{C_S \cdot \lambda} \qquad (10)$$

with which the largest contrast transfer and therefore best image contrast is achieved. We will use the Scherzer focus in order to resolve the delocalization zone between amorphous Si and monocrystalline Si, and of course to see atomic columns.

An example for a CTF is given in Figure 15:

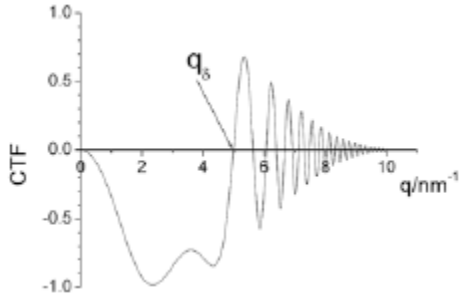

Figure 15: Example for a CTF with applied Scherzer focus.

Measurement of the resolution limit

Nowadays it is easily possible to measure the resolution limit of a TEM using the so-called 'Young fringes'. Experimentally, Young fringes can be achieved by shifting the image while image acquisition. When observing the live transformed images Young fringes become visible. An example is shown in Figure 16.

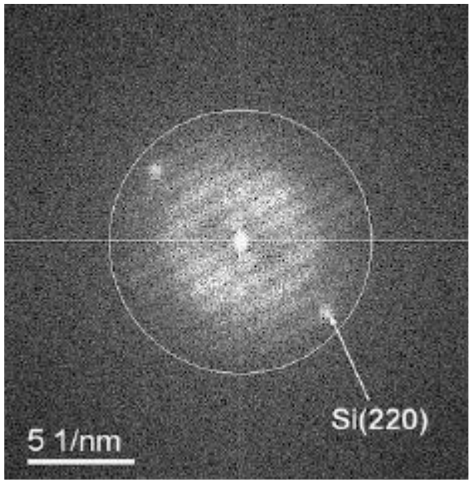

Figure 16: Young fringes in a Fourier transformed image.

The circle shown in Figure 16 shows the informational limit of the microscope, which is a reciprocal value of the spatial frequency $= \frac{1}{q}$, which the Young fringes reach. In that manner, we will measure the resolution limit of our microscope.

Tasks for the report

1. Briefly explain the alignment procedure (without theoretical information).
2. Explain the process of aligning the objective stigmatism using FFT images on amorphous films.
3. Explain how the values 'informational limit' and 'point resolution' can be understood in relation to the Scherzer-focus. Where can those values be found in the CTF?
4. Show and explain the difference between the images with Gaussian and Scherzer focus (with respective FFTs).
5. Calculate the 'informational limit' of our TEM. Make use of Young's fringes.
6. Take a diffraction pattern of monocryst. Si, index it and calculate the zone axis.
7. Calculate the lattice parameter of Si using a HRTEM image and compare it to literature.
8. Compare one BF-image of the sample polycrystalline part with two differently oriented DF images using beam tilt.
9. Explain and perform the experimental steps to measure the specimen thickness using CBED patterns (see next chapter for the theory).

Recommended literature to read

[1] D B. Williams and C. Barry Carter. Transmission electron microscopy: a textbook for materials science. New York, Spinger, 2009.
[2] L. Reimer, H. Kohl Transmission electron microscopy: physics of image formation New York, NY: Springer, 2008
[3] B. Fultz, J. Howe Transmission electron microscopy and diffractometry of materials. Berlin; New York: Springer, 2008
[4] J Bozzola; L D Russell. Electron microscopy: principles and techniques for biologists. Boston, Jones and Bartlett, 2006.

Tutor:

Robert Lawitzki
Office: 2Q11
Robert.Lawitzki@mp.imw.uni-stuttgart.de +49 711-685-61911

Transmission Electron Microscopy 3 (TEM): Simulation and Image Analysis

Introduction

One of the main challenges, when working with a TEM, is the interpretation of the obtained micrographs or diffraction patterns. In most cases, an intuitive interpretation is not possible and accompanying simulations or post analysis using certain software is necessary. In this part of the lab, you will work with various software packages that are used in the TEM community: *JEMS* is the most common used software for simulation of TEM diffraction patterns and images. We will use it for the simulation of the CTF and different monocrystalline and polycrystalline diffraction patterns. Furthermore, we will work with *CrysTBox*, a software that can read and analyze experimental TEM data and *ImageJ*, a free but very powerful tool for image processing.

Convergent Beam Electron Diffraction

This theory part will focus on the convergent beam electron diffraction (CBED) technique, a technique that allows for instance to measure the thickness of a sample; an information which may be important for calculating the density or volume fraction of precipitates but also for correct interpretation of diffraction patterns. CBED patterns contain far more crystallographic information than parallel beam diffraction patterns, but their interpretation needs more experience and pre knowledge.

In contrast to conventional selective area diffraction (SAD) techniques which uses a parallel illumination, convergent beam electron diffraction (CBED) operates with a converging electron beam. In other words, in SAD the electron beam transmitting the sample is parallel and therefore illuminates a relatively large area of 1-10 µm in diameter. However, with CBED, the beam is converged on a small spot on the specimen (less than 500 nm nanometer in diameter). Depending on the convergence angle, diffraction spots appear now as discs with a certain diameter (cf. Figure 17 b). Furthermore, Kikuchi lines are presented in a CBED-pattern, which provide crystallographic information about the specimen. Supplementary to SAD, CBED can be used to obtain information from much smaller volumes enabling a very localized crystallographic analysis. Various information like the specimen thickness, unit cell and precise lattice parameters, the crystal system and crystal symmetry can simultaneously be evaluated. In case of CBED the convergence semi-angle varies

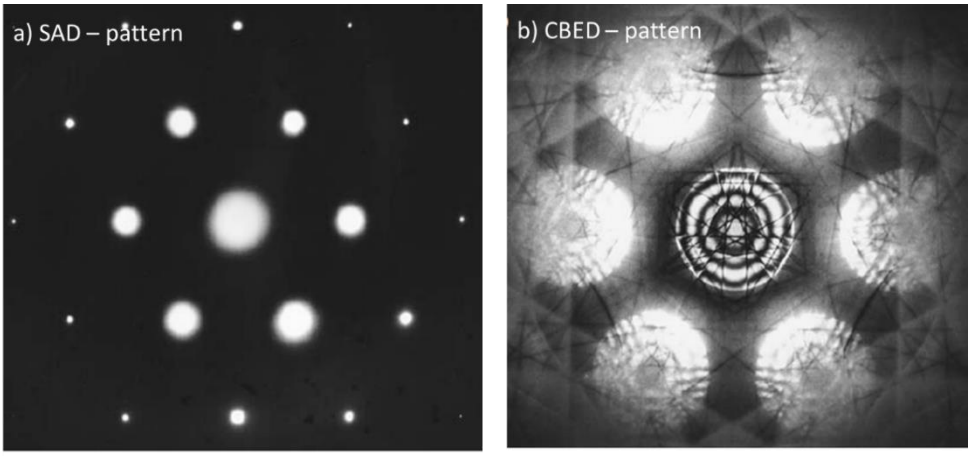

Figure 17: a) SAD pattern from (111) Si showing the first few orders of diffraction spots and no visible Kikuchi lines b) CBED pattern from the same position. The small spots are now discs that show strong contrast variations within the discs as well as diffused Kikuchi bands. (Williams, Carter book p.325)

from 0.1° to 0.5° and depends on the C2 aperture used. The disc size can be magnified by changing the camera length. Figure 17 shows a clear comparison of what is observed in a SAD pattern and in a CBED pattern.

Due to the coexistence of image features in a CBED pattern they can be considered as a diffraction-imaging pattern. Crystal defects such as dislocations, but also the thickness of the sample modify the pattern and create typical artefacts. When you record a CBED pattern of a crystal tilted exactly to zone axis, the disk usually will contain concentric fringes known as Kossel-Möllenstedt (K-M) fringes (see Figure 17 b). These fringes contain thickness information and therefore, the sample thickness can be measured exactly at the beam position. In practice, thickness measurements are usually not performed in a zone-axis condition. Instead, two-beam conditions with only one strongly excited hkl reflection are used. By this, the CBED disks contain parallel oscillations as shown in Figure 18 a), which simplify their analysis. In order to understand the information generated by these fringes, one has to look closer at their distances. These are linked to the extinction length of a crystal in a certain orientation (for further information we advise to take look in TEM bible of Williams and Carter).

In order to analyze the thickness using such a CBED pattern, one has to follow a certain procedure: First one has to measure the distances between the middle of the central bright fringe and each of the dark fringes in the diffracted disk. The central bright fringe is at the exact Bragg condition with the deviation parameter s = 0. The fringe spacings correspond to angles $\Delta\theta_i$, and from these spacings you can calculate the deviation parameter s_i for the i^{th} fringe (where i is an integer) from the equation

$$S_i = \lambda \frac{\Delta\theta_i}{2\theta_B d^2}, \qquad (10)$$

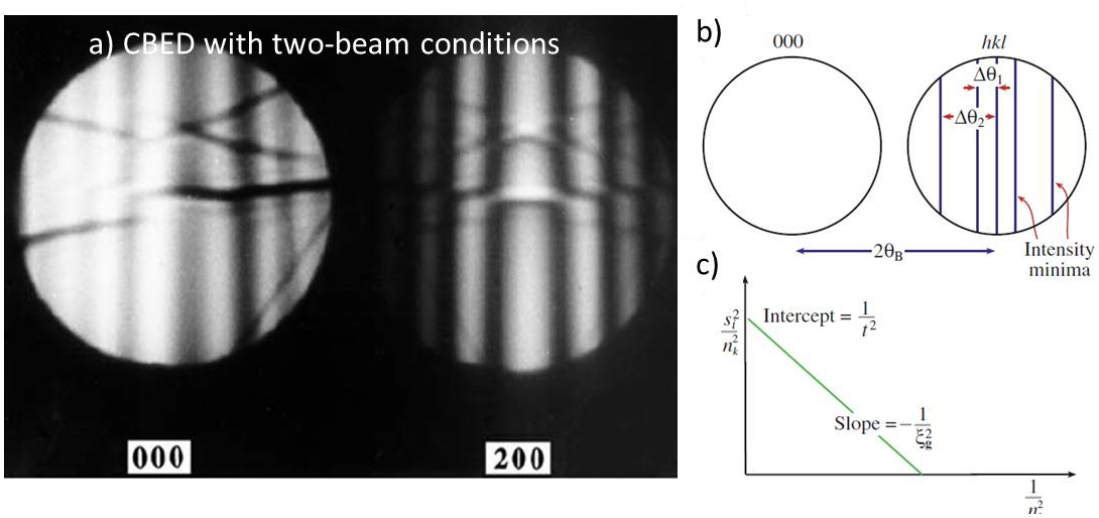

Figure 18: a) Parallel Kossel-Mollenstedt fringes in a CBED pattern from pure Al taken under two beam conditions with a (200) reflection. b) Measurement of K-M fringes. Measurement of n_k distances between the dark fringes $\Delta\theta_i$ and calculation of the deviation parameters s_i, then c) plot of $(s_i/n_k)^2$ versus$(1/n_k)^2$ represents a straight line. By extrapolating to the ordinate to find t^{-2}, the thickness t can be calculated.

where θ_B is the Bragg angle for the diffracting hkl plane and d is the hkl interplanar lattice spacing. The thickness of the sample can then be determined using the relation between the extinction distance ξ_g and the specimen thickness t

$$\frac{s_i^2}{n_k^2} + \frac{1}{\xi_g^2 n_k^2} = \frac{1}{t^2}\,, \tag{11}$$

where n_k is an integer with n=1 for the first fringe. When the extinction distance ξ_g is not known the graph shown in Figure 2c) is used by arbitrarily assigning the integer n = 1 to the excitation error s_1. If the obtained graph is a straight line as shown in the figure, then the thickness value and extinction length value can be calculated easily from the intercept and slope.

Tasks for the report:

1. Identify with the help of *JEMS*, the crystallographic structure of different experimental polycrystalline and monocrystalline diffraction patterns (Si-diamond and Ni_3Al-$L1_2$) and index the patterns, which will be given to you on the laboratory day. (Extra task: Identify and explain the origin of the diffraction pattern in file “Ni3Al_What_Happened_Here.dm3”).
2. Investigate the relationship between the voltage (U) and the spherical aberration coefficient (C_s) on the contrast transfer function. Draw two diagrams, where you plot the point to point resolution as a function of different voltages and C_s (at least 4 points for each plot). Discuss in which conditions the maximum

resolution can be achieved. What is the influence of the chromatic aberration on the CTF?

3. Use the Bloch wave simulation in the JEMS program to generate a thickness-defocus map of $LiFePO_4$ (battery cathode material in spinel structure). Start from zero defocus, end at four times the Scherzer focus of the CM200-FEG instrument, thickness should range from 5 to 50 nm.
4. Simulate the images of a triple layer Ni/Ni_3Al_{10nm}/Ni (layers perpendicular to the beam). What happens if the ordered layer is put at different height within the foil?
5. By using *CrysTBox* and *ImageJ*, investigate the thickness from the CBED patterns that are given to you. Different CBED patterns were obtained along a wedge shaped sample. Plot a graph of the thickness versus the position where the pattern was taken (distance in the sample) and evaluate the shape of the wedge.

Recommended literature to read

[1] D B. Williams and C. Barry Carter. Transmission electron microscopy: a textbook for materials science. New York, Spinger, 2009.
[2] JEMS manual: http://www.jems-saas.ch/Home/jemsWebSite/jems.html
[3] CrysTBox manual: https://www.fzu.cz/~klinger/crystbox.pdf

Tutor:

Franziska Maier
Office: 2Q11
Franziska.Maier@mp.imw.uni-stuttgart.de +49 711-685-61911

Lift-out procedure using a Focused Ion Beam (FIB)

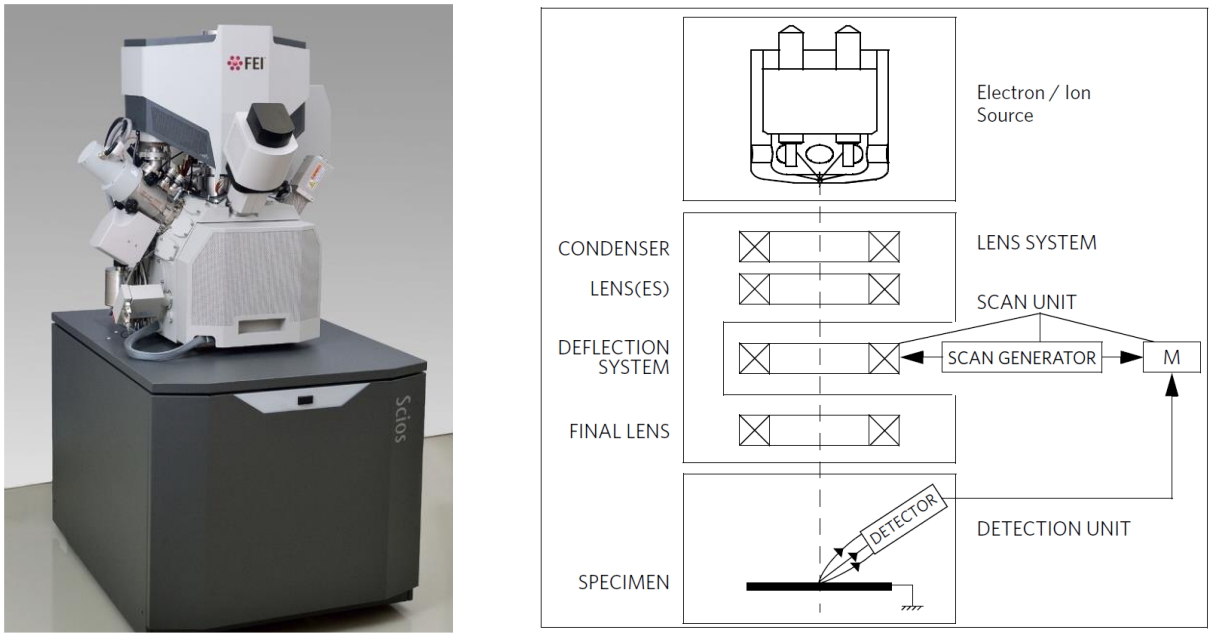

Figure 19: Left: FEI Scios™ DualBeam™ field ion and scanning electron microscope (FIBSEM). Right: Schematic overview of the column of a dual beam microscope.

The FEI Scios is a dual beam microscope consisting of a Scanning Electron Microscope (SEM) and a Focused Ion Beam (FIB) system. The SEM is capable of achieving magnifications over 100 000× and high resolution images. The FIB system allows fast and precise milling or deposition of material as well as high resolution imaging.

Imaging

A beam of electrons or ions is emitted within a small spatial volume with a small angular spread and selectable energy. The beam enters the lens system consisting of several electromagnetic and/or electrostatic lenses and exits to hit the specimen surface. The scan generator signal, fed to the deflection systems, moves the beam in a raster pattern over the specimen area. This signal, modulated by the detection system signal produces the onscreen imaging of the specimen surface. Particles striking the specimen interact with atoms of the sample surface in various manners. The electron beam produces electrons and X-Ray photons (see SEM experiment), the ion beam produces ions, electrons and X-Ray photons. A detector picks up the particles or photons, converts them into a digital signal which is then sent to the control PC and shown on the monitor. A schematic overview of the column is shown in Figure 19.

Detector Types and Application

The Scios can be equipped with several detectors. A list of available detectors is given in Table 2. For this course the operator will use the Everhart-Thornley Detector (EDT) and the Ion Conversion and Electron Detector (ICE).

Table 2: Available detectors for FEI Scios microscopes. SE = secondary electrons, SI = secondary ions, BSE = back scattered electrons, TE = transmitted electrons, S = standard, O = optional, L = Low Vacuum model only.

Detector Name	Tag	Vacuum Mode	Detected Signal	Note
Everhart-Thornley	ETD	HiVac	SE (tunable energy) / BSE	S
T1	T1	HiVac / LoVac	BSE (for OptiTilt and OptiPlan column Use cases)	S
T2	T2	HiVac / LoVac	SE (for OptiTilt and OptiPlan column Use cases)	S
Low Vacuum	LVD	LoVac	SE	S
CCD camera	CCD		light, infra-red light	S
External	EXT		detector-dependent	S
T3	T3	HiVac	SE (for OptiTilt and OptiPlan column Use cases)	O
Ion Conversion and Electron	ICE		electron beam: SE / BSE ion beam: SE / SI	O
Retractable Directional Backscattered (DBS)	ABS / CBS	HiVac	BSE	O
Directional Gaseous Analytical (05/2015)	GAD-ABS / GAD-CBS	LoVac	BSE	O, LM
Retractable Annular STEM	STEM 3 STEM 3+	HiVac	TE	O

Specimen Preparation and Manipulation

The Specimens are mounted on the Standard Stub Holder shown in figure 2. Once the specimen chamber is evacuated, a region of interest is selected and the stage is moved to the eucentric position using the SEM. Electron beam-induced deposition of a protective Pt-layer is used to protect the region of interest from the Focused Ion Beam. The stage is tilted to 52° and a second, thicker Pt-layer is deposited using ion beam-induced deposition (see Figure 20). The geometric relationships of stage, electron- and ion-column and detectors are shown in Figure 21.

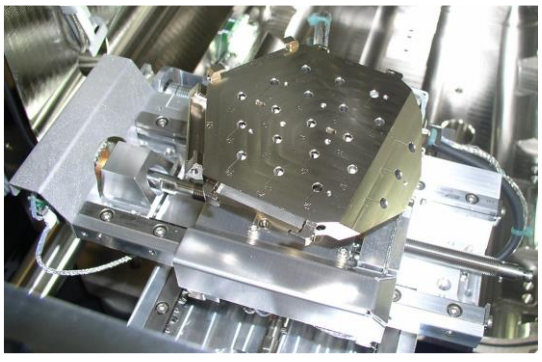

Figure 20: Standard Stub Holder (Stage).

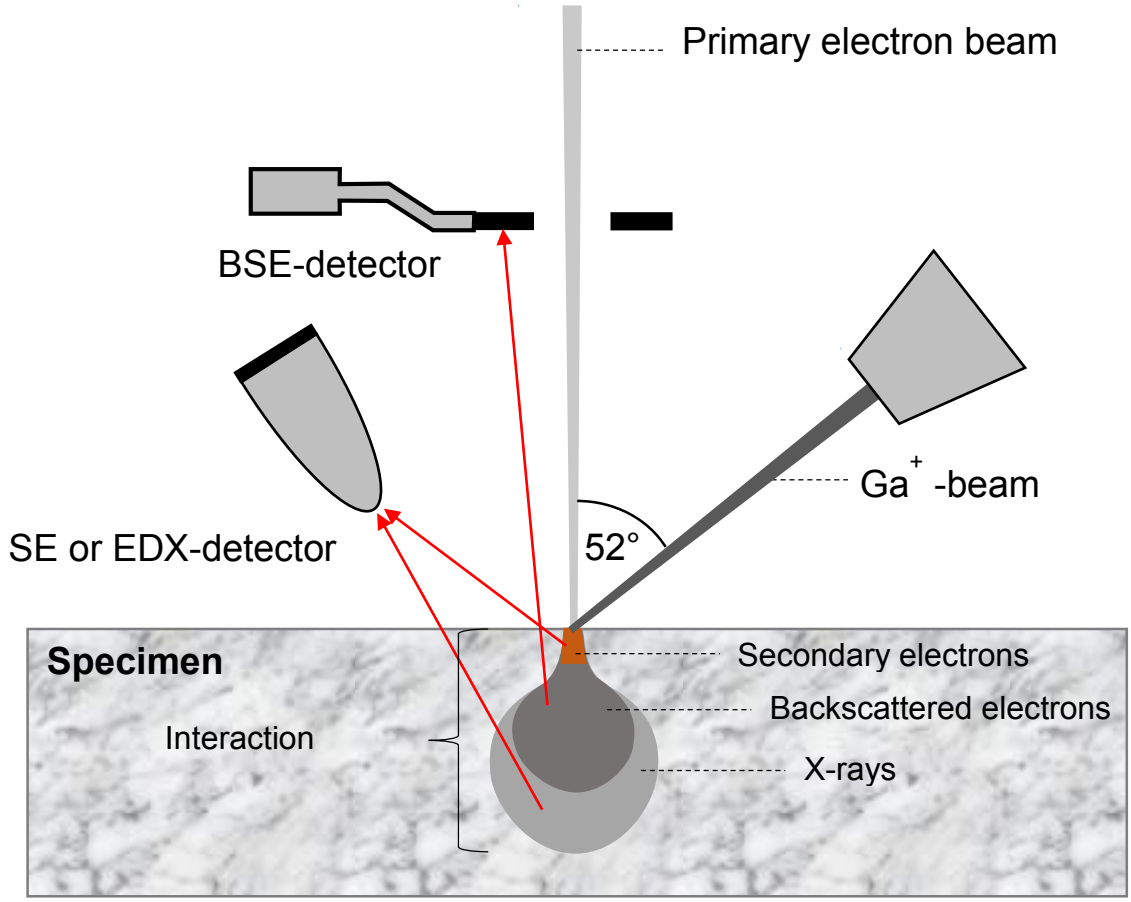

Figure 21: Geometric relationships of stage, electron- and ion-column.

Procedure of cutting a lamella

- Cross sectioning patterns are cut on both sides of the protective layer using a high ion current (Figure 22 left and right).

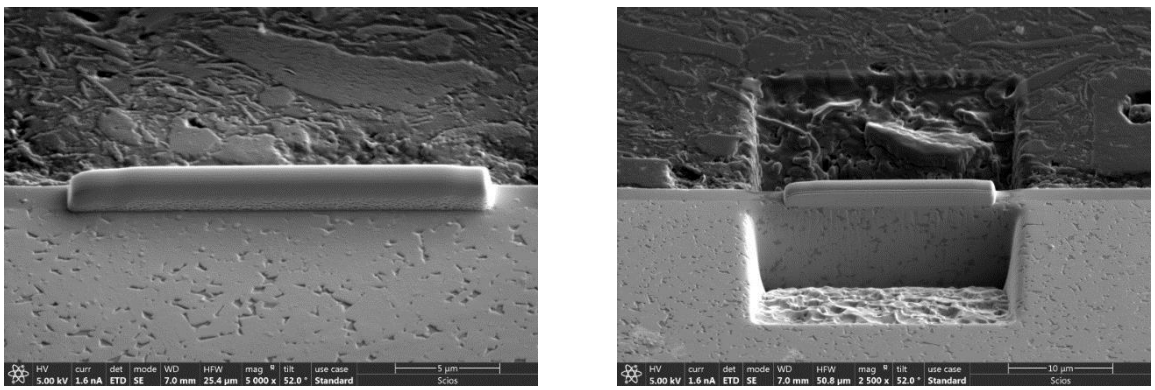

Figure 22: Left: Protective Pt-layer on a region of interest. Right: Cross sectioning patterns cut on both sides of a protective Pt-layer.

- The lamellas surfaces are cleaned using cleaning cross sectioning patterns (Figure 23).

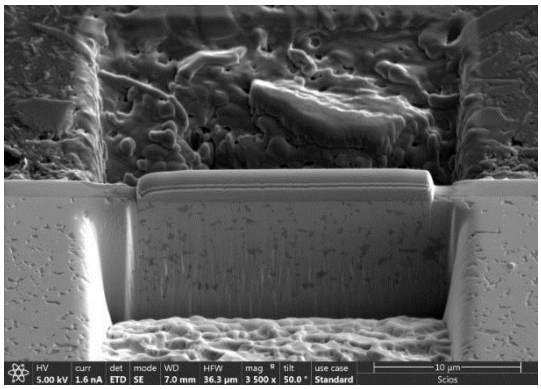

Figure 23: Lamella with cleaned surfaces.

- The stage is tilted to 10° and an L-shaped undercut is performed.
- The stage is tilted to 0° and the micro manipulator is inserted to its parking position.
- The micro manipulator is moved to the lamella and attached by deposition of Pt.
- The Lamella is cut loose (Figure 24) and removed from the specimen.

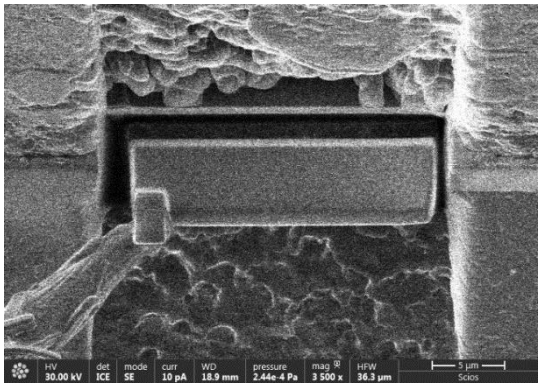

Figure 24: Specimen lamella attached only to the micro manipulator.

The lifted-out lamella will further be used to prepare specimens for atom probe tomography and transmission electron microscopy. These processes will be explained by the operator during the course.

Tutor:

Yug Yoshi
Office: 2Q11
Yug.Joshi@mp.imw.uni-stuttgart.de +49 711-685-61905

Sample preparation for EBSD

EBSD (Electron Backscatter Diffraction) is a characterization method to determine the microstructure, grain orientation, size distribution and texture of materials. (See instructions for EBSD laboratory)

This equipment works complementarily within SEM (Scanning Electron Microscopy), by accelerating the electron beam onto the sample surface, the back-scattered electrons are generated inside the surface and the diffracted Kikuchi pattern which corresponds to individual crystal orientation is detected.

Suitable sample preparation plays a crucial role to get a successful EBSD result. As shown in Figure 25, the mechanically polished sample (a) which has a lot of scratches on the surface shows low quality of EBSD results, see the orientation indexing map (b), compared to the electropolished sample (c and d). The requirement for EBSD measurement is that the specimen should have a perfectly smooth and flat surface (roughness below 50 nm) without deformation and damage.

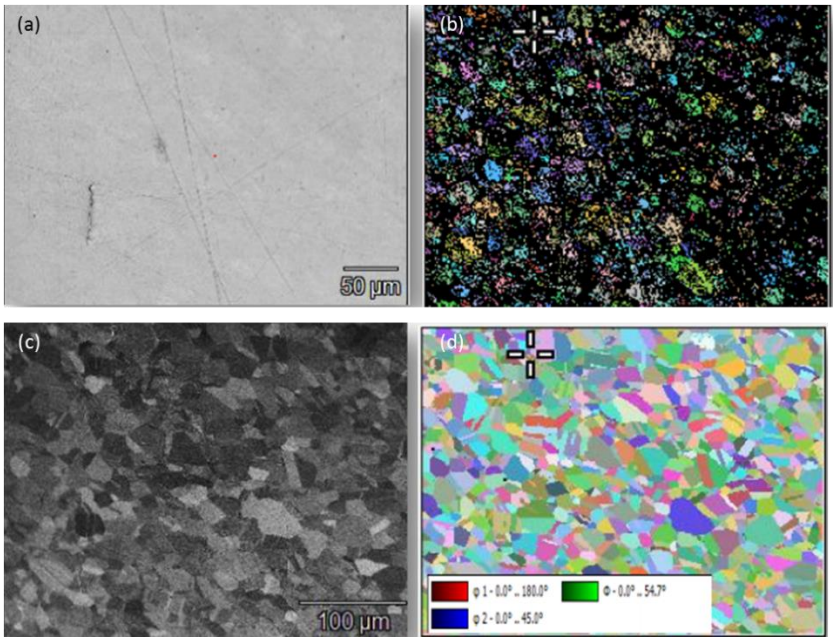

Figure 25: Comparison between mechanically polished specimen (a and b) and Electopolished specimen (c and d). (a) and (c) are the SEM image. (b) and (d) show the orientation image map. (MAGCIS – A Novel Method for EBSD surface preparation, n.d.)

There are several methods to produce the specimen for EBSD measurement: Electrochemical-polishing, Ion Beam Preparation and Plasma cleaning. For this practical course, the electrochemical-polishing method is applied. A pure copper foil

(Alfa Aesar, 99.9 % purity and 0.127 mm thick) will be electropolished using nitric acid solution as an electrolyte for this experiment.

Procedure

Cu foil is bended slightly and flattened again punched into Ø 3 mm disks at least 10 times. Then the Cu disks undergo a heat treatment using a small annealing oven (MILA-5000 Mini-lamp). The heating parameters (which will be given to you on the experiment day) can be chosen selecting a temperature and a time. A simple heat treatment requires the selection of 4 stages, including initiating (starting temperature), increasing temperature (heating rate), holding temperature (annealing temperature and time) and cooling down to ambient temperature.

Put the specimens into the oven crucible. To start the annealing oven, turn on the water cooling and vacuum pump and wait until the vacuum condition is reached around ($4.0 – 7.0 \times 10^{-2}$) mbar. Then introduce the argon gas up to ($3.0 – 4.0 \times 10^{-1}$) mbar and start the heating. When specimens are cooled down, close the vacuum pump valve and open the oven chamber by argon gas flow smoothly.

After heat treatment the samples are mechanically polished. The disks are glued on a metal disk using epoxy glue then by using the SiC grinding papers (1200 and 4000) the samples are mechanically polished by hand and/or automatic grinder for both side. Thereafter, polished specimens are rinsed with acetone and alcohol via ultra-sonication to remove remaining glue and impurities.

The next step is electrochemical polishing using an electrolyte containing 700 ml Methanol (99.9 % purity) and 350 ml of nitric acid (65% purity). By using liquid nitrogen, the electrolyte is cooled down to – 35 to – 40°C and the temperature is checked with a thermometer. Next, the specimen is mounted in specimen holder in between two platinum rings to optimize the polishing in the central region. They are fixed in the polishing cell contacting the platinum conductors to make an electrical connection to the polishing circuit.

Then select the etching method via control unit and move to User mode and select mode 11. CU and the 1. EBSD. There are parameters (Voltage, Temperature, Polishing time, flow rate) which can be modified in order to find better polishing conditions. Depending on the quality of specimen after mechanical polishing step, the parameters for electrolytic polishing might be varied.

When the electrolytic polishing is completed, the specimen is directly introduced into the water bath to be separated from the holder and cleaned in ethanol. Finally, using

silver conductive paint, the specimens are glued on the electron microscopy sample holder to make EBSD measurement later.

Tasks

1. Describe the experimental procedure.

2. Write down the parameters used for heat treatment and electropolishing and specify the optimum parameters by checking with optical microscope.

Literature

[1] “MAGCIS – A Novel Method for EBSD surface preparation," Thermo Fischer, [Online]. Available: https://tools.thermofisher.com/content/sfs/brochures/WS52725-MAGCIS-EBSD-Webinar.pdf.

Tutor:

Yoonhee Lee
Office: 2R14
Yoonhee.Lee@mp.imw.uni-stuttgart.de +49 711-685-61907

Electron BackScatter Diffraction (EBSD)

The aim of this laboratory is to get familiar with the electron backscatter diffraction (EBSD) technique using a scanning electron microscope (SEM) and to get a first insight to the interpretation and evaluation of EBSD-data. To be more precise, differently heat treated electropolished Cu-discs will be analyzed in terms of grain sizes and the development of the microstructure using a FEI Scios™ DualBeam™ field ion and scanning electron microscope (FIBSEM) (cf. Figure 19) which is additionally equipped with an EBSD camera system and the required software for evaluation.

Introduction

EBSD in SEMs is the most widely used technique which links the specimens' microstructure and crystallography, also known as microtexture. By the use of electrons as a source of radiation (compared to x-rays or neutrons), it is possible to create a probe size down 20-50 nm, smaller than the size of the microstructural units themselves. In modern instruments, this probe can automatically scan the specimen's surface pixel by pixel in order to generate, capture, store and index diffraction patterns with a rate of up to 500 patterns per second and thus enables fast data collection rates.

In order to maximize the proportion and minimize the energy spread of backscattered electrons, the specimen is usually tilted in way that there is an angle of 20° between incident electron beam and specimen surface. The resulting diffraction (or Kikuchi) pattern is captured with the EBSD camera or a phosphorous screen (cf. Figure 26 a). To understand the principles of orientation determination it is important to understand the formation of a Kikuchi pattern.

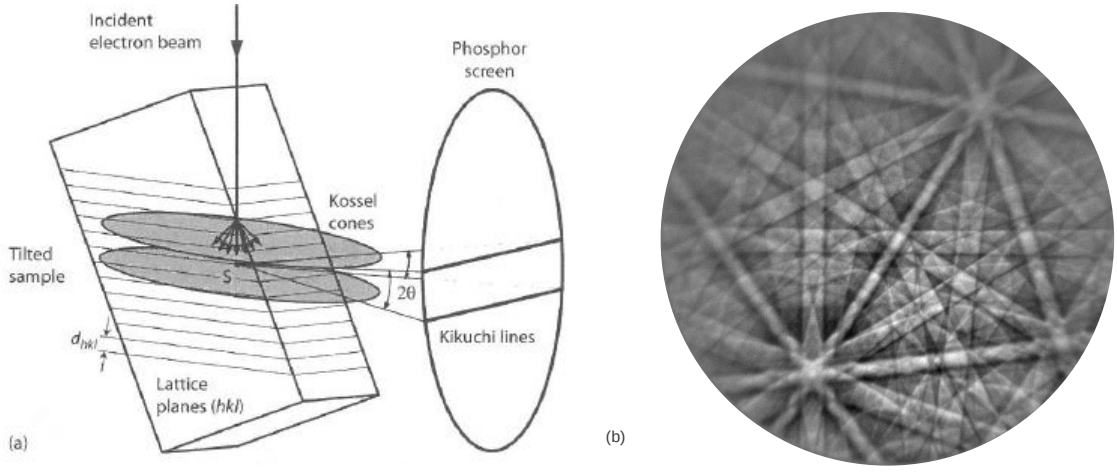

Figure 26: Formation of backscattered Kikuchi patterns by EBSD in SEMs: a) Origin of Kikuchi lines from tilted specimen [1]. b) EBSD pattern from Ni (20 kV).

Kikuchi patterns: Kikuchi lines in SEM are a phenomenon that occur when backscattered electrons get diffracted. Since electrons are backscattered in every direction, they can undergo Bragg diffraction at every set of lattice planes and thereby form a Kossel cones corresponding to a distinct crystallographic lattice plane. Since electrons can be diffracted from both sides of the atomic planes, two cones per lattice plane can be observed in form of two lines or a band (cf. Figure 26 b). The intersection of these lines with another pair of lines is called a zone axis and is related to a specific crystallographic direction in the crystal. The orientation of the zone axis [*uvw*] can be derived from the cross product of the intersecting bands (h_1,k_1,l_1) × (h_2,k_2,l_2).

The width of a pair of lines is linked to the Bragg angle θ which is inversely related to the lattice plane spacing *d,* given by the Bragg equation for a certain wavelength λ:

$$n\lambda = 2d \sin\theta \tag{12}$$

This means, a wider lattice plane spacing or larger acceleration voltage will result in a smaller distance between the pair of Kikuchi lines [2]. The observed Kikuchi pattern is a gnomonic projection of the angular relationships in the crystal onto a flat surface. Thus, distances near the pattern center scale linearly with the projection angle and areas far from the pattern center will be geometrically distorted.

Indexing (determining the crystallographic indices) of the Kikuchi pattern is the first step in each EBSD pattern analysis. This can be done either manually (by comparison with standard patterns), semiautomated (a user marks the position of the bands and a computer indexes them) or fully automated, which means that the pattern recognition and indexing is completely done by software. The latter one uses the *Hough transform* to convert lines into points which can be detected more easily by computer codes.

The next step is the *determination of the crystallographic axis* of the sample in reference to the beam direction. In order to keep the mathematics simple, the case that the beam direction is parallel to the samples' normal direction ND is further considered only (cf. Figure 27a). Then the angles α_1, α_2 and α_3 (cf. Figure 27b) can be easily determined from the screen/camera to sample distance d_{ss} and the distances d_i between the pattern center (here: point ND) and the surrounding three nearest indexed poles q^1, q^2 and q^3:

$$\tan\alpha_i = \frac{d_i}{d_{ss}} \tag{13}$$

The resulting sample normals (*h*,*k*,*l*) can now be calculated and normalized by:

$$\begin{pmatrix} q_1^i \\ q_2^i \\ q_3^i \end{pmatrix} \cdot \begin{pmatrix} h \\ k \\ l \end{pmatrix} = \cos\alpha_i \cdot \sqrt{\left(q_1^i\right)^2 + \left(q_2^i\right)^2 + \left(q_3^i\right)^2} \quad . \tag{14}$$

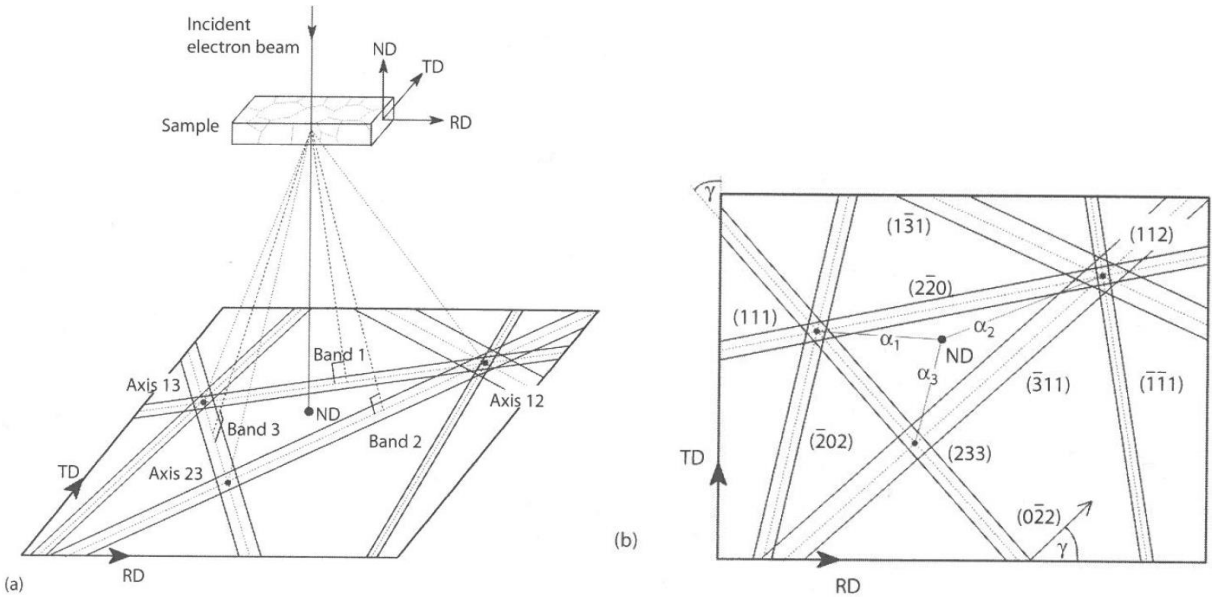

Figure 27: Scheme that illustrates the evaluation of a Kikuchi pattern with the samples' normal direction ND parallel to the incident beam direction [1]: a) Link between the reference frame of the specimen and the Kikuchi pattern. b) Indexed Kikuchi pattern corresponding to figure a).

The derivation of the full rotation orientation matrix (or the Euler Angles) that links the macroscopic specimen coordinate system to the crystal coordinate system would require the determination of one further reference axis (e.g. the rolling direction RD). This is more complex and not always necessary and will thus not be treated in more detail. In this experiment, the reference axis of the specimen will not be changed (no specimen tilt or rotation) during mapping of the sample and thus orientation relationships or misorientations can still be calculated.

Important abbreviations & keywords in EBSD analysis used by the software:

PF – A pole figure is the projection of the intersection of a grain's normal vector with a reference sphere (pole) onto a plane with regard to an external reference frame.

IPF – Contrary to the PF, the inverse pole figure represents the projection of the orientation of the specimen coordinate system into the crystal coordinate system. Usually IPFs are visualized in form of stereographic triangles.

Euler Angles – The first set of numbers in the status bar are the Euler angles in Bunge notation. These three angles describe the orientation of the crystal with respect to the sample coordinate frame. (hkl)[uvw] – The first set of indices describe the crystal plane parallel to the surface of the sample and the second set give the crystal direction parallel to the sample reference direction.

IQ – The image quality parameter describes the quality of the pattern. It is derived from the Hough transform. It gives some indication as to how well the Hough is able to detect the bands.

CI – The confidence index describes how reliable the indexing solution is. If this value is low (< 0.1), data points need to be treated

Fit – The fit describes the overall average angular mismatch between the overlaid bands and the bands detected by the Hough transform. Lower values are better. A large value (> 3°) often indicates a problem with the calibration of the system.

All the before mentioned information can be color coded and used for visualization.

Experimental procedure

I. Mount the specimen stub to the 70°-pretilt sample holder and fix it on the stage.
II. Pump the instrument and take a photo with the navigation camera.
III. Start the electron gun (20 kV and 0.8 nA) and find a flat area on your specimen for the analysis.
IV. Adjust the specimen to a working distance between 13-17 mm to have maximum intensity in the center of the EBSD camera.
V. Start the *Team* Software and insert the EBSD camera (be very careful, it may not touch the specimen!).
VI. Optimize gain and exposure time without binning (1x1) to obtain the best Kikuchi pattern.
VII. Use the *Calibration* tab and determine the pattern center and camera to sample distance. Tune the diffraction pattern to optimize the fit.
VIII. Use the automatic ”Fast” optimization mode, in order to find the best imaging conditions for a fast EBSD mapping with sufficient image quality. Use image processing filters to further optimize your pattern
IX. Map an area of e.g. 250x250 µm² or 350x350 µm² (ensure that many grains are included) and use a step size between 0.5 µm and 1 µm. Then start the mapping.

Analysis

I. Export your data to the OIM software.
II. Depending on the quality of the data, apply a dilation cleanup.
III. Evaluate your data according to the tasks given below. A brief introduction to the software will be given on the experiment day.

Tasks for the report

- Manually evaluate the Kikuchi pattern that was obtained without using binning. Index both, the most important Kikuchi line pairs and zone axes (compare with figures in appendix for help). Consider the crystal structure of your specimen and that the pattern is distorted. Calculate the crystallographic indices (*hkl*) of the samples' normal under the assumption that the beam normal is parallel to the normal direction of the sample. The diameter of the phosphor screen of the EBSD camera is 34 mm.
- Evaluate the grain sizes of the differently heat treated Cu specimens.
- Compare and report the development of microtexture using different visualization techniques ("kernel average misorientation", "local orientation spread", "inverse pole figures" or "grain reference deviation – angle").
- Determine which kind of grain boundary (low/high energy, twin or a certain CSL boundary) is dominating.

References

[1] V. Randle and O. Engler, *Introduction to Texture Analysis: Macrotexture, Microtexture and Orientation Mapping*. Taylor & Francis, 2000.

[2] J. M. Joseph Goldstein, Dale Newbury, David Joy, Charles Lyman, Patrick Echlin, Eric Lifhshin, Linda Sawyer, *Scanning Electron Microscopy and X-Ray Microanalysis*. Springer Science + Business Media New York, 2007.

Further Information about EBSD:

http://www.ebsd.com/

Tutor:

Dr. Gábor Csiszár
Office: 2Q17
Gabor.Csiszar@mp.imw.uni-stuttgart.de +49 711-685-61912

Appendix

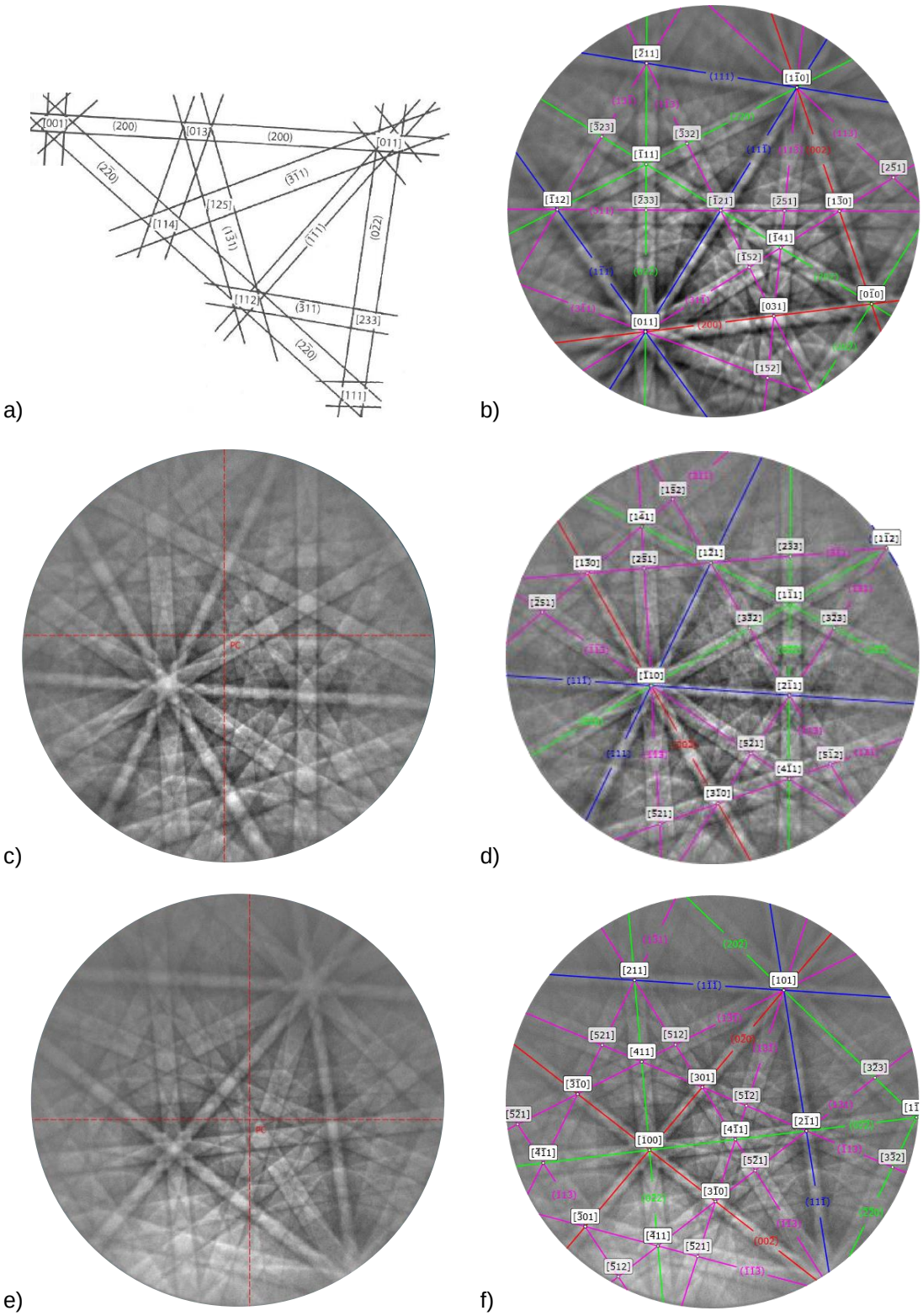

Figure 28: a) Standard Kikuchi map for fcc (one stereographic triangle) [1]. B) Indexed Kikuchi pattern referring to the pattern shown in figure 1 b). c) and e) Kikuchi pattern of further grains from Ni (20 kV); the pattern center PC is highlighted in red. d) and f) Indexed Kikuchi pattern shown in figure c) and d).

Atom Probe Tomography (APT): Measurement

Introduction

Atom probe tomography (APT) is a technique which allows the chemical analysis of a small volume with atomic resolution. By applying a high electric field to a needle shaped specimen, atoms are ionized and evaporated. This process is called field evaporation. A standing DC voltage is applied to the specimen, which is not sufficient to evaporate atoms of the tip in a controlled way. By applying high voltage pulses to an extraction electrode or laser pulses to the tip apex, the evaporation of one atom is triggered. The ion is then accelerated towards a position sensitive detector and the required time to reach the detector is measured. From the time of flight and the impact position of the detector, the evaporated volume can be reconstructed. Comparing to conventional high voltage pulsing, the laser pulsing method makes it possible to measure insulating materials, which is not possible with HV pulses because of the poor electric conductivity.

In this experiment the laser-assisted micro-electrode tomographic atom probe (METAP) is used to investigate different samples produced by electropolishing and FIB lift-out.

Instrument Components

Vacuum & Cooling

For an APT-measurement ultra-high vacuum conditions are required, so that no residual gas atoms interfere the measurement. The custom built atom probe of our institute consists of three UHV chambers (see Figure 30) for measurement, storage and exchange of the specimen. Each chamber is pumped by a turbomolecular pump which are backed by a prevacuum buffer. The working pressure within the measurement chamber is in the order of 10^{-10} mbar. In order to measure such low pressures, an ionization gauge is needed, which consists of a filament, an anode grid and an ion collector. The filament is heated and emits electrons, which are accelerated to the anode and thus ionize residual gas atoms/molecules on their way. The ions are then collected and the ion current is measured, which is proportional to the pressure.

For a good spatial resolution and the reduction of noise, the specimen needs to be cooled down to cryogenic temperatures (20 – 80 K). This is done by a He closed cycle cryostat, which works by compressing and expanding He gas repeatedly. Additionally,

the cooling head acts as a cryopump and thus improves the vacuum by one order of magnitude.

Extraction Electrode

In contrast to the electric TAP, the laser-assisted TAP uses an extraction electrode with an aperture diameter in the µm-range, therefore the name METAP (micro-electrode TAP). This leads to the enhancement of the electric field of about a factor of two, which reduces the required applied voltage in order to generate sufficient electric fields. This also improves the mass resolution, since the energy spread is reduced due to lower voltages.

Laser System

In laser-assisted atom probe, the evaporation is triggered thermally. The laser increases the temperature locally by 100 – 300 K. The used laser system “Impulse” by ClarkMXR is a femtosecond laser based on Yb-doped fibers with a fundamental wavelength of 1030 nm. The pulse width can be adjusted between 220 fs and 10 ps with a selectable repetition rate between 100 kHz and 24.7 MHz. While its higher harmonics with wavelengths 515 nm and 343 nm can be generated. For our measurements we will be using UV-laser pulses with a frequency of 200 kHz. Lenses direct and focus the beam into the needle’s apex through a quartz glass window. The laser power can be adjusted to a desired value with the help of a λ/2 plate. The laser spot position is controlled by a piezo-driven mirror and is monitored by a CCD camera that is also suitable to detect UV wavelength.

Detector System

In order to reconstruct the measured volume, a position sensitive detector is required. The used detector consists of a 120 mm Roentek delay line (DL) electrode and two microchannel plates (MCP) with a diameter of 80 mm in Chevron geometry. The MCPs serve as a signal amplifier. The MCPs have µm-sized channels which are densely packed. Additionally, the channels are inclined at a small angle relative to the surface of the plate to increase the gain. When an ion hits one of those channels, a cascade of electrons is produced which amplifies the signal strongly.

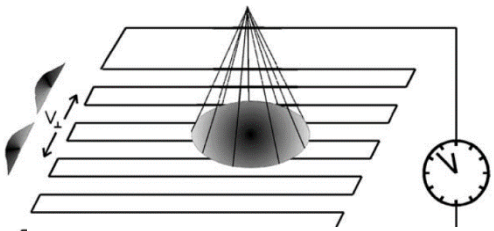

Figure 29: Scheme of a delay-line readout [1].

Typically, the electrodes of the delay line are meander-shaped (see Figure 29). Once the electron cloud generated by the MPCs hits the DL, a signal travels to both ends of the line. The position can now be determined by measuring the time difference which the signal needs to reach each end of the line. This gives for example the *x*-coordinate of our signal. For the *y*-coordinate a second DL is placed underneath the first, perpendicular oriented to it.

The detection efficiency amounts only to about 50 %, since ions which hit the area between the channels of the MCP are lost. This means that only every second atom is detected. Newest detectors provide efficiencies up to 80 %.

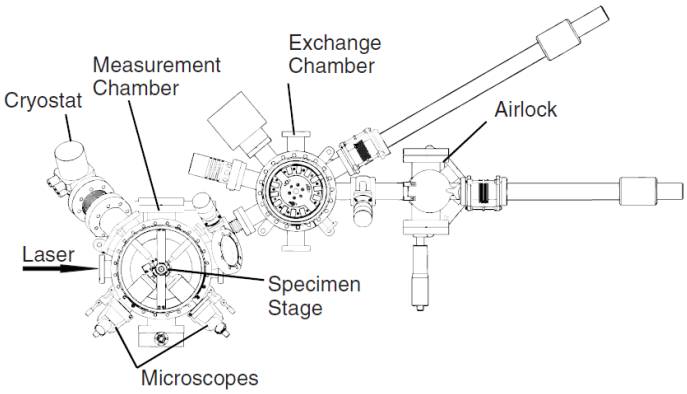

Figure 30: Construction of the METAP in top-view [2].

The ion identification is done by measuring the time of flight (ToF), that the ion needs to reach the detector. Once the laser pulse starts, a start time signal is started and is terminated when an ion hits the detector.

Experimental Procedure

An introduction how to operate the tool correctly will be given on the experiment day, the following guide describes the main steps to conduct the experiment:

- Switch on cryostat (will already be done, takes approx. 2 hours to cool down).
- Vent airlock and remove sample holders.
- Put samples into sample holder at the correct position (tip should be on the upper edge of “O” on the scale bar, will be explained during the experiment).
- Put sample holders back into the airlock.
- Close the lid and start the pump for the airlock.
- Wait approx. 20 min for the pressure to establish in the airlock.
- Open valve to the exchange chamber, transfer samples and close the valve again.
- Open the valve to the measurement chamber, transfer one sample and close the valve again.
- Press IMG in order to check the pressure, the measurement should be performed at $p < 3\times10^{-10}$ mbar.
- Wait approx. 20 min for the sample to adapt to the temperature.

- Lower the electrode with the upper vertical bar, position the tip beneath the center of the electrode with the two horizontal bars.
- In the meantime, the laser can be started, make sure that the windows of the measurement chamber are covered.

CAUTION: We're working with a laser of the category 4 which is the most dangerous class. Under no circumstances you should look directly into the beam or the beam path, even reflections or diffuse light can cause permanent eyesight loss! Never put your hand into the beam, this can lead to serious flesh burns and/or could cause clothing to catch fire! Don't wear any reflecting jewelry during handling of the laser!

- The calibration will be done by the supervisor for the reasons above!

Now the actual measurement can be started:

- Make sure that IMG is off! Otherwise the detector would be damaged!
- Check that the window is covered!
- Switch on following buttons on the device in this order:
  - HV (high voltage) → Detector → Electronics.
- Start the software "TAPCONTROL" (restart software if it is already open).
- Go to settings and create saving file.
- Set parameters:
  - Ratio: 0.5 – 1.4 %
  - Refresh Rate: 0.2 s^{-1}
- Check box next to "Detector" → detector is starting, wait until it reached 100%.
- Press "open shutter" on the control screen of the laser.
- Press start on the computer → laser should be now visible.
- Position the laser spot onto the very top of the tip → use the "agilis" tool to move the spot.
- Activate base and automatic voltage control → measurement starts running.
- Proper evaporation start depends on the material and the initial tip radius, usually around 2-3 kV you get the main peaks.
- Adjust the position of the laser in such a way that you get a high evaporation rate, low noise in the mass spectra and a homogenous detector image.

The measurement is finished if the tip breaks or the maximum voltage is reached. Stop the measurement following these steps:

- Press "stop".
- Stop the detector.
- Uncheck automatic voltage control and base, reduce base voltage to 0.

- When detector has shut down, close the program.
- Switch off the buttons on the device: press Electronics → Detector → HV.
- Bring electrode completely up again.
- Close the shutter of the laser.

Tasks for the report

- Summarize the experimental procedure.
- Write down the parameters you used for the experiment (pressure, temperature, laser power, etc.).
- At which voltage did the main peaks appear? Did the voltage reach a plateau?
- Note how many atoms were measured.
- How does the positioning of the laser influence the mass spectrum?
- How did the detector image look like during the measurement?

References

[1] O. Jagutzki et al., Nucl. Instr. Meth. Phys. Res. A 477 (2002) 244.

[2] R. Schlesiger et al., Rev. Sci Instrum. 81 (2010) 043703.

Tutors:

Ahmed Mohamed Abdelkarim and Jianshu Zheng
Office: 2Q11
Ahmed.Mohamed@mp.imw.uni-stuttgart.de +49 711-685-61911
Zheng.Jianshu@mp.imw.uni-stuttgart.de +49 711-685-61904

Reconstruction of Atom Probe Data

Introduction

Atom Probe Tomography offers an unprecedented ability to map the positions of individual atoms in three dimensions to reveal the structural arrangement of the atoms inside a material [1]. In this laboratory, we will learn how the atoms are processed and displayed from the original atom probe measurement data, and what material information we can get from them. All the work will be done by the Scito reconstruction software on a Windows computer with large memory.

Reconstruction Method

Reconstruction means determining the real 3D coordinates of the atoms from the 2D positions received from a position sensitive detector. First, we need to define what kind of element we get via clarifying the mass-to-charge-state ratio $\frac{m}{n}$ of every single atom by using the Newton's equation of motion [2]:

$$M = \frac{m}{n} = 2e(U_B + \alpha U_P)\frac{(t_{flight} - t_0)^2}{L_{flight}^2} \tag{15}$$

where L_{flight} is the flight distance, t_{flight} is the measured time-of-flight of the ions, t_0 is the time shift which occurs by transporting the electrical signal, U_B and U_P are base voltage and pulse voltage applied on the specimen, α is the voltage pulse fraction, and e is the elementary charge of the electron.

To determine the atomic coordinates of the specimen, different approaches can be used. In commercial software and also in this experiment, the reconstruction is based on the "point-projection model" (see :).

The electric filed applied on a tip, E, can be described as [1]:

$$E = \frac{U}{\beta R} \tag{16}$$

where U is the total voltage applied on the tip, R is the apex radius, and β is the so-called field factor, which considers the influence of tip geometry and so the change of the electric field.

By assuming that the ionized atoms leave the surface of the sample in a straight trajectory, they form an image on the detector that corresponds to a magnified image

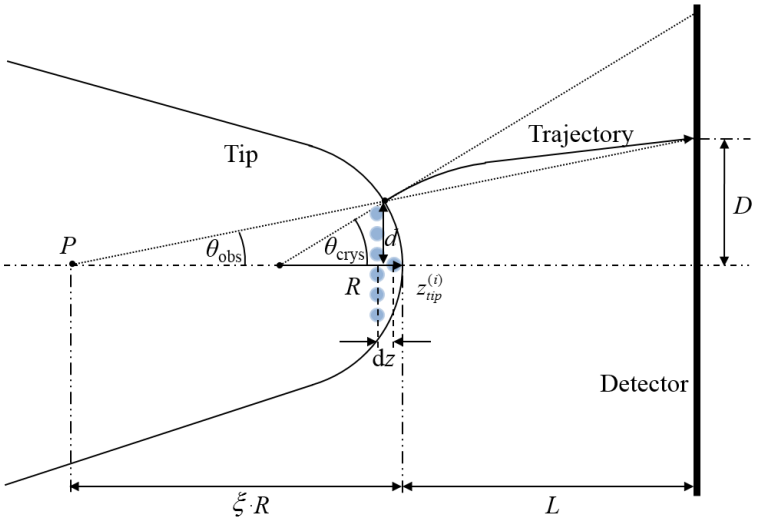

Figure 31: Schematic view of the geometric considerations [3].

of the sample surface. The magnification is calculated by the intercept theory. As the flight path, *L*, is much greater than the radius of curvature of the specimen *R*, the magnification, M_{proj}, can be written as [3]:

$$M_{proj} = \frac{D}{d} \approx \frac{L}{\xi R} \tag{17}$$

ξ is the image compression factor. Since the trajectories of the ionized atoms don't follow the theoretical field lines which are expected to be perpendicular to the tip surface, ξ gives the deviation from the ideal case. For small angles, the image compression factor ξ thus can be defined as the ratio of θ_{crys}, the angle between two crystallographic directions imposed by the theoretical crystalline structure of the material, to θ_{obs}, the angle between the poles observed on the projected image [3]:

$$\xi = \frac{\theta_{crys}}{\theta_{obs}} \tag{18}$$

The tip coordinates x_{tip} and y_{tip} are calculated out of the measured detector coordinates X_D and Y_D by [1, 2, 4, 5, 6]:

$$x_{tip} = \frac{X_D}{M_{proj}} = X_D \frac{R\sin(\theta_{crys})}{D} = \frac{X_D}{\sqrt{X_D^2 + Y_D^2}} R\sin(\xi\theta_{obs}) \tag{19}$$

$$y_{tip} = \frac{Y_D}{M_{proj}} = Y_D \frac{R\sin(\theta_{crys})}{D} = \frac{Y_D}{\sqrt{X_D^2 + Y_D^2}} R\sin(\xi\theta_{obs}) \tag{20}$$

where $$D = \sqrt{X_D^2 + Y_D^2} \tag{21}$$

To determine the *z* coordinate, Bas method is widely used (see :). As ions are removed from the tip atom-by-atom and layer-by-layer, the distance between the specimens tip and detector become larger. Hence, for each new ion added to the reconstruction, this emitting surface is incrementally shifted by a small quantity d*z*, then the *z* should be described as [5, 6]:

$$z_{tip}^{(i+1)} = z_{tip}^{(i)} + dz \tag{22}$$

In : , we can deduce $z_{tip}^{(i)}$ by [5, 6]:

$$z_{tip}^{(i)} = R\left(1 - \cos\left(\xi\theta_{obs}\right)\right) \tag{23}$$

For each ion hitting the detector with an area A_d, the *z*-coordinate is changed by the small distance *dz* given for small fields of view by [5, 6]:

$$dz = \frac{\Omega_i}{\zeta \cdot A_e} = \frac{\Omega_i \cdot M_{proj}^2}{\zeta \cdot A_d} = \frac{\Omega_i \cdot L^2}{\zeta \cdot A_d \cdot \xi^2 \cdot R^2} = \frac{\Omega_i}{U_i^2}\left[\frac{(L\beta E)^2}{\zeta \cdot A_d \cdot \xi^2}\right] \tag{24}$$

where A_e is the emitter cross-sectional area equivalent to A_d, Ω_i is the atomic volume of the *i*th ion in the phase under analysis, and ζ is the detection efficiency of the single-ion detector. The fourth and fifth expressions above come from applying Eq. (17) and then Eq. (16). U_i is the total voltage applied to the specimen, in order to field evaporate the *i*th ion.

Required Data Files

After successful measurement with the atom probe, you will receive a data file with the extension .raw in binary format. This file contains the unprocessed dataset of each measured atom (Table 3) i.e. the coordinates of the impact position of the ion on the position-sensitive detector, the time of flight, the applied voltages, and the ion's position in the sequence of detected ions.

Furthermore, a parameter file (.par) and alloy file (.aly) are required. The parameter file contains machine and tip geometry parameter, while the alloy file assigns the measured atoms their elements. For this experiment a standard parameter and alloy file are given, which are then adjusted accordingly during reconstruction.

Table 3: Information contained in raw file from an atom probe measurement [4].

Parameter	Notes
UBase	Standing voltage (V)
UPulse	Additional voltage pulse (V)
PosX	Detector X-Pos (ns)
PosY	DetectorY-Pos (ns)
TOF	Time of flight (ns)
Time	Time Marker
Puls	Number of pulses since measurement start. (Currently always 0)

Using reconstruction software "Scito"

Open the software "Scito" and click "New Project" in order to choose a save directory and load your raw, parameter and alloy file. Click on the header "Raw - Data" in order to see the voltage evolution of the measurement. In this step you can filter the measurement data by modifying the different settings on the left side, e.g. voltage range, data range or radial detector area.

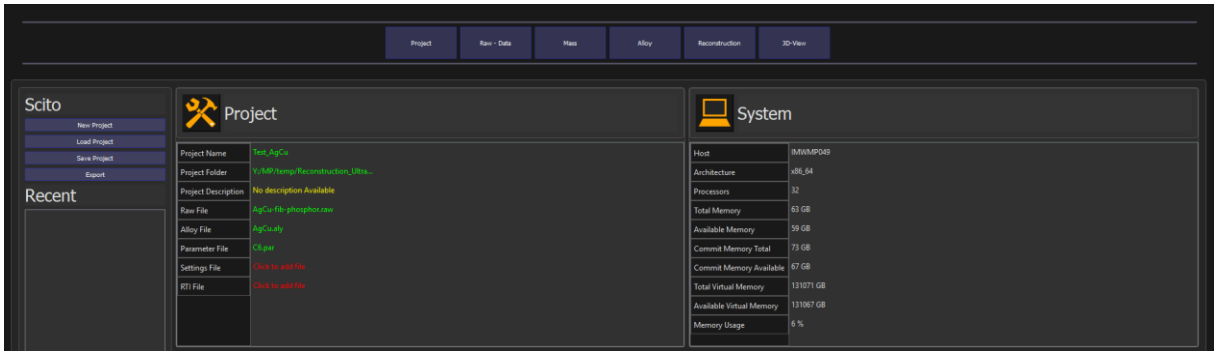

Figure 32: Overview of Scito interface.

Next, the mass spectrum is evaluated. Change therefore to the header "Mass" and click on "Calculate Mass" in order to plot the mass spectrum. Check that the mass peaks are at the correct positions, otherwise adjust flight length and time-of-flight offset accordingly.

After adjustment of the mass spectrum, the mass windows need to be defined. Change to "Alloy". By clicking on "Add Definition" you define an element and assign its color. With "Add Window" you can specify the minimum and maximum ranges of a mass window for a defined element. Furthermore, the charge state needs to be given. The same procedure is done in the case of molecules. After all mass windows are set, click "Apply", which will display a brief overview of the overall composition. Additionally, you

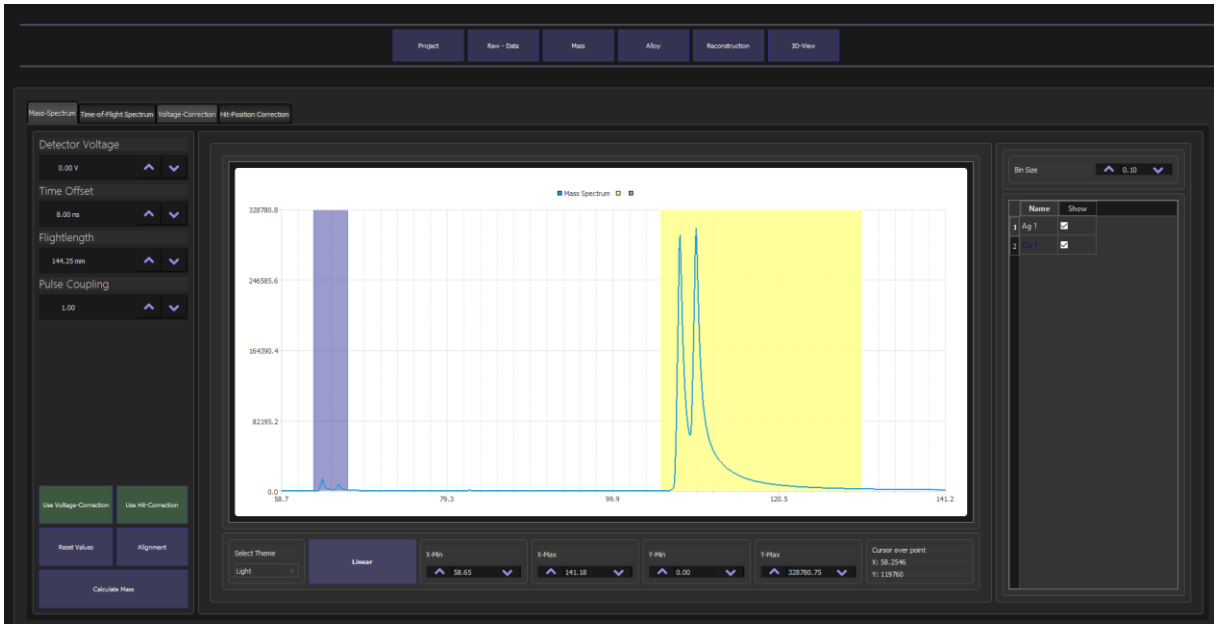

Figure 33: Mass spectrum with set mass windows.

can go back “Mass” and check the mass windows again, since they are now displayed in the mass spectra. Changes can be done by either moving (mouse wheel + click) or adjusting the ranges (right click + dragging) of the windows.

After all windows are set, you can go to the “Reconstruction” section. There, you can choose different reconstruction algorithms. For our purposes only the “Taper Geometry” algorithm is used. It allows adjustment of the evaporation field by changing curvature radius R, field compression factor β and taper angle α. The values are adjusted in such a way that the evaporation field fits literature data (see periodic table in appendix). Decreasing R will result in increasing field, while changing α will change the slope of the curve. After proper calibration, you can start the analysis.

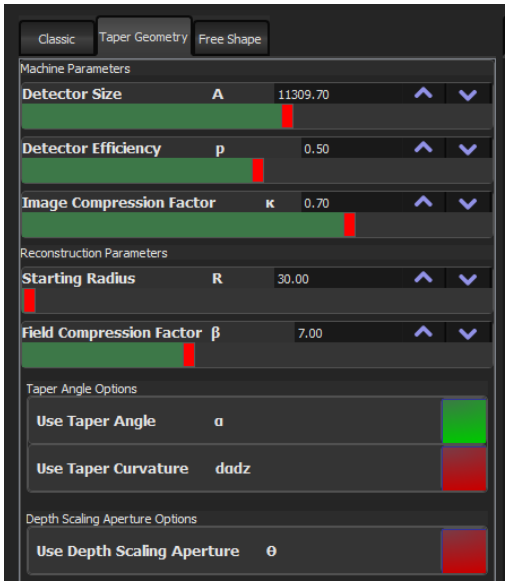

Figure 34: Adjustable parameters for "Taper Geometry" algorithm.

.

Tasks

Obtain information from the mass spectra and reconstructed 3D model about the composition and distribution of the atoms. Use geometry filters to crop a smaller amount of data (e.g. box or cylinder), isosurfaces for atomic distributions and 1D-composition profiles.

References

[1] B. Gault, M.P. Moody, J.M. Cairney, et al. *Atom Probe Microscopy*. Springer New York, **2012**.

[2] P. Stender. *Thermal stability investigation of a nanocrystalline Iron-Chromium multilayer system.* Ph.D. dissertation in Westfälischen Wilhelms-Universität Münster, **2010**.

[3] Script of materials science lab course: *Field ion microscopy and atom probe tomography*, Chair of Materials Science, University of Stuttgart, **2016**.

[4] P. Stender. *Atom Probe Tomography Reconstruction: A Short Manual*, **2012**.

[5] M.K. Miller, R.G. Forbes. *Atom-Probe Tomography: The Local Electrode Atom Probe*. Springer New York, **2014**.

[6] D.J. Larson, T.J. Prosa, R.M. Ulfig, et al. *Local Electrode Atom Probe Tomography: A user's guide*. Springer New York, **2013**.

Tutors:

Rüya Duran (2Q11) and Helena Solodenko (2Q15)

Rueya.Duran@mp.imw.uni-stuttgart.de +49 711-685-61904
Helena.Solodenko@mp.imw.uni-stuttgart.de +49 711-685-61982

Appendix A: Atom Probe's Periodic Table of Elements